Table 1.   Primers Sequences Used for RT-PCR

Gene	Forward primer	Reverse primer
Human *PTHrP*	5'-GCTGTGTCTGAACATCAGCT-3'	3'-TTTGTACGTCTCCACCTTG-5'
Human *RANKL*	5'-CCAGCATCAAAATCCCAAGT-3'	3'-CCCCAAAGTATGTTGCATCCTG-5'
Human *IL-6*	5'-AAATTCGGTACATCCTCGAC-3'	3'-CAGGAACTGGATCAGGACTT-5'
Human *ACTB*	5'-AAACTGGAACGGTGAAGGTG-3'	3'-TCAAGTTGGGGGACAAAAAG-5'
Mouse *Pthrp*	5'-CGGTTTGGGTCAGACGATG-3'	3'-TTCCCGGTGTCTTGAGTG-5'
Mouse *Rankl*	5'-ATGATGGAAGGCTCATGGT-3'	3'-CCAAGAGGACAGAGTGACTTT-5'
Mouse *Opg*	5'-CTGCCTGGGAAGAAGATCAG-3'	3'-TTGTGAAGCTGTGCAGGAAC-5'
Mouse *Il-6*	5'-GAGGATACCACTCCCAACAGACC-3'	3'-AAGTGCATCATCGTTGTTCATACA-5'
Mouse *Tnf-α*	5'-GGCATGGATCTCAAAGACAACC-3'	3'-CAGGTATATGGGCTCATACCAG-5'
18SrRNA	5'-GTAACCCGTTGAACCCCATT-3'	3'-CCATCCAATCGGTAGTAGCG-5'

lated ST2 cells onto a 24-well plate (5×10^4 cells/well) and cultured them in α-modified minimum essential medium containing 10% FBS, 1×10^{-8} mol/L 1,25-dehydroxyvitamin D_3 (Sigma-Aldrich), and 1×10^{-7} mol/L dexamethasone (Sigma-Aldrich) for 24 hours. Then, mouse bone marrow cells (5×10^5 cells/well) isolated from the femora and tibiae of 6-week-old C57BL/6 mice were cocultured with ST2 cells in 0.5 ml of α-modified minimum essential medium containing 10% FBS, $1 \times 10^{[8}$ mol/L 1,25-dehydroxyvitamin D_3, and 1×10^{-7} mol/L dexamethasone in the presence or absence of CM derived from each cancer cell line. The culture medium was replaced every other day. After coculturing for 6 days, the cells were fixed in 10% buffered formalin and stained with tartrate-resistant acid phosphatase for osteoclast identification by incubation with 0.1 mol/L sodium acetate buffer (pH 5.0) containing AS-MX phosphate (Sigma-Aldrich) and red violet LB salt (Sigma-Aldrich) in the presence of 50 mmol/L sodium tartrate (Sigma-Aldrich). Tartrate-resistant acid phosphatase-positive cells that contained more than three nuclei were identified as osteoclasts and were counted.

Xenograft Experiments of HSC3 Cells into Athymic Mice

HSC3 cells (5×10^5 cells/injection) were injected onto the periosteal region of the parietal bones in athymic mice using a 1-ml syringe after the periosteum was scratched once with the syringe needle. Three weeks after the transplantation, the calvarial region was dissected and fixed with 4% paraformaldehyde. Soft X-ray photographs were taken after fixation. The tissues were embedded in paraffin after decalcification with 10% EDTA at 4°C for 10 days. The sections were used for histological observation including immunohistochemical analysis for RANKL, human IL-6, and mouse IL-6. The experimental procedures were reviewed and approved by the Animal Care and Use Committees at Tokyo Medical and Dental University.

Statistical Analyses

Statistical analyses were performed using Student's t-test and Pearson's correlation coefficient. $P < 0.05$ was considered significant. The data are the mean ± SEM of independent replicates.

Results

Expression of IL-6 and PTHrP mRNA in Primary Human OSCC

The clinical and pathological data for the 43 cases of primary OSCC used for microarray analysis are summarized in Table 2. As shown in Figure 1A, mRNA expression of *IL-6* varied among the cancers and the oral epithelium adjacent to the cancers. Although only two SCC specimens expressed *IL-6* mRNA at extremely high levels, the average fluorescence intensity in the cancer cells was 199.82 ± 427.67 and that in the adjacent oral epithelium was 302.92 ± 367.88 without a significant difference between these two groups (Figure 1A). In contrast, most of the cancer tissue specimens overexpressed *PTHrP* mRNA (average fluorescence intensity 735.58 ± 769.59) compared with the adjacent epithelial specimens (average fluorescence intensity 20.59 ± 12.80) (Figure 1B), demonstrating significantly higher expression level of *PTHrP* mRNA in the cancer tissues than in the adjacent epithelium ($P < 0.000001$). These results imply that many of the OSCC specimens overexpressed *PTHrP* mRNA, but few overexpressed *IL-6* mRNA, compared with the adjacent epithelium specimens.

Expression of IL-6 at Bone Invasive Region in Gingival SCC

To confirm the expression profile of IL-6 by microarray analysis, we examined immunohistochemically the distribution of IL-6-positive cells at the bone-invasive regions in gingival SCC. Although IL-6 was expressed in some tumor cells and oral epithelia adjacent to the tumors, expression varied among the cases studied. More importantly, the fibroblastic cells at the tumor-bone interface also expressed IL-6 (Figure 2, A and B). Incubation of the sections with nonimmunized IgG exhibited no positive reactions (data not shown). The fibroblastic cells at the bone-invasion region also expressed RANKL (Figure 2C). These findings were noted in 10 of 13 specimens examined; we further analyzed the distribution of the positive cells in these 10 specimens by histomorphometry. Because the percentages of RANKL- and IL-6-positive cells among the total number of fibroblasts in a given area varied among the specimens examined (RANKL-positive cells, 11.4 to 65.9%; IL-6-positive cells, 25.1 to 84.1%),

Table 2.   Clinical and Histological Characteristics of the 43 Cases of Primary Human Oral Squamous Cell Carcinoma Used for Microarray Analysis

Case	Sex	Age	Primary site	T	N	Histological grade*
1	M	56	Lower gingiva	2	0	Moderately
2	M	55	Upper gingiva	2	0	Well
3	M	56	Upper gingiva	2	0	Well
4	F	64	Lower gingiva	4a	1	Well
5	M	77	Lower gingiva	2	2b	Poorly
6	M	78	Lower gingiva	2	1	Well
7	M	71	Lower gingiva	3	2b	Well
8	M	60	Lower gingiva	4	2b	Moderately
9	M	57	Upper gingiva	4a	1	Poorly
10	M	52	Lower gingiva	4a	2b	Moderately
11	M	66	Lower gingiva	2	0	Well
12	F	66	Upper gingiva	2	0	Moderately
13	M	72	Lower gingiva	2	0	Well
14	M	68	Lower gingiva	4a	2b	Moderately
15	F	66	Tongue	2	0	Moderately
16	M	80	Tongue	2	0	Well
17	M	30	Tongue	2	0	Well
18	F	60	Tongue	2	0	Well
19	M	59	Tongue	3	0	Moderately
20	M	54	Tongue	1	0	Well
21	M	43	Tongue	2	0	Moderately
22	M	46	Tongue	2	0	Well
23	M	58	Tongue	2	0	Well
24	M	66	Tongue	1	2b	Moderately
25	M	61	Tongue	1	2c	Moderately
26	M	70	Tongue	3	1	Moderately
27	M	37	Tongue	2	3	Poorly
28	M	73	Tongue	2	0	Poorly
29	M	32	Tongue	3	0	Moderately
30	F	54	Tongue	2	2b	Moderately
31	M	60	Tongue	4	2c	Moderately
32	M	53	Tongue	2	2b	Moderately
33	M	62	Buccal mucosa	1	0	Well
34	F	74	Buccal mucosa	2	1	Moderately
35	M	71	Buccal mucosa	3	2b	Poorly
36	M	58	Floor of mouth	2	0	Well
37	M	58	Floor of mouth	3	0	Moderately
38	M	66	Floor of mouth	3	1	Moderately
39	M	59	Floor of mouth	4	1	Moderately
40	M	67	Floor of mouth	4	1	Well
41	M	72	Hard palate	1	0	Moderately
42	F	81	Retromolar pad	1	0	Well
43	M	68	Retromolar pad	2	0	Moderately

M, male; F, female; T, tumor; N, node.
*Histological grading: well, well differentiated SCC; moderately, moderately differentiated SCC; poorly, poorly differentiated SCC.

we tested the correlation between the numbers of each cell type per specimen. The number of RANKL-positive fibroblastic cells correlated significantly with the IL-6-positive fibroblastic cells at the tumor-bone interface ($r = 0.935926$, $Y = 0.8115X − 28.644$, $P < 0.0001$) (Figure 2D), suggesting that the RANKL and IL-6 synthesized by stromal cells interact closely. The RANKL-positive cells are located close to the bone surface and osteoclasts (Figure 2C). The distribution of IL-6-positive cells at the tumor-bone interface varied depending on the areas examined in each case; the cells were located close to the cancer nests at some areas (Figure 2B) and to the bone and osteoclasts at other areas (Figure 3, B–D).

To further characterize the IL-6-positive cells, we performed dual immunohistochemical analysis using fluorescence-labeled antibodies. Numerous fibroblastic cells expressed IL-6; furthermore, IL-6 expression was also observed in cancer cells located at the periphery of cancer nests (Figure 3, B–D). Several osteoclasts were also IL-6-positive (arrows in Figure 3, A and C). Many IL-6-positive fibroblastic cells coexpressed vimentin (Figure 3B); furthermore, the number of IL-6-positive fibroblastic cells was very high compared with the number of IL-6-positive B cells (Figure 3C) and macrophages (Figure 3D), suggesting that fibroblastic cells dominantly produce IL-6.

Human Oral Cancer Cells Secrete Factors That Stimulate Osteoclast Formation by Inducing RANKL Expression in Stromal Cells

We performed *in vitro* experiments to examine whether CM derived from the various cancer cell lines could induce RANKL expression in stromal cells. The CM derived from all cancer cell lines, with the exception of A549,
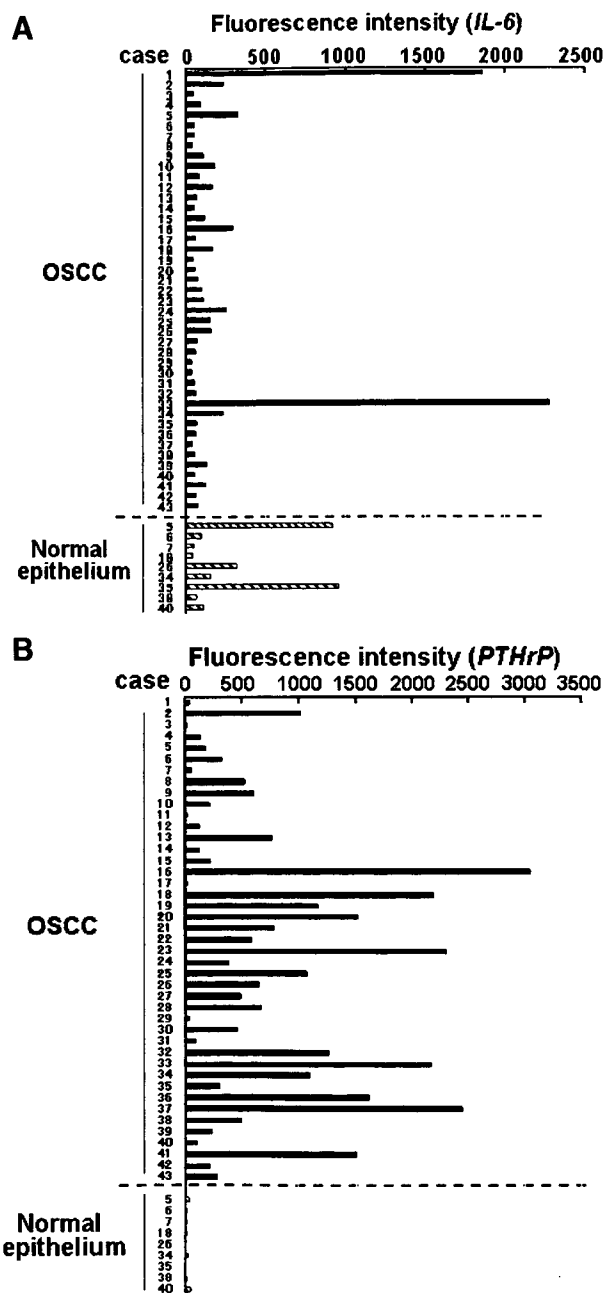
A

B

Figure 1. Expression of *IL-6* and *PTHrP* in OSCC. Expression profiles of *IL-6* (**A**) and *PTHrP* mRNA (**B**) in 43 primary human OSCC specimens assessed by microarray analyses as described in *Materials and Methods*. Expression levels in normal epithelium are also shown at the bottom of **A** and **B**. The fluorescence intensity, which was the absolute value of fluorescence intensity in each case, was used to indicate the mRNA expression level.

stimulated *Rankl* mRNA expression in ST2 cells (Figure 4A). The CM derived from BHY and HSC3 cells markedly increased this expression. In addition, the CM derived from oral cancer cell lines (BHY, Ca9, and HSC3) significantly enhanced *RANKL* mRNA expression in mesenchymal stem cells isolated from human bone marrow (Figure 4B). However, none of the CM significantly altered *Opg* mRNA expression (data not shown).

We also investigated the effects of CM on osteoclast formation by using a mouse coculture system. As shown

in Figure 4C, the CM derived from all of the cancer cell lines increased the number of tartrate-resistant acid phosphatase-positive osteoclasts. These results suggest that oral cancer cell lines as well as cancer cells originating from nonoral regions stimulate osteoclast formation by inducing RANKL expression in stromal cells.

IL-6 and PTHrP Synthesized by Cancer Cells Are Involved in RANKL Expression and Osteoclast Formation

We then investigated the expression levels of IL-6 and PTHrP in various cancer cell lines. As shown in Figure 5A, all of the cell lines expressed *PTHrP* mRNA at substantial levels, whereas only BHY and HSC3 cells, which are derived from OSCC, expressed *IL-6* mRNA at substantial levels. These results suggest that many OSCC cells express *PTHrP*, but only limited numbers of OSCC express *IL-6*.

To explore the roles of IL-6 and PTHrP, we next examined the effects of neutralizing antibodies against mouse IL-6 receptor[32] and human PTHrP[33] on *Rankl* mRNA expression in ST2 cells. Both antibodies inhibited BHY-CM-induced *Rankl* mRNA expression (Figure 5B) in a dose-dependent manner (Supplemental Figure S1, see http://ajp.amjpathol.org). The maximum concentration of PTHrP antibody used (10 μg/ml) almost completely blocked PTHrP-induced cAMP production in ROS 17/2.8-5 cells.[33] Similar results were obtained with HSC3-CM (data not shown). Because BHY and HSC3 cells expressed *IL-6* mRNA at substantial levels, we tested the effects of these antibodies on *Rankl* mRNA expression by using CM derived from Ca9 cells (Ca9-CM), which expresses *IL-6* mRNA at undetectable levels (Figure 5A). As expected, human PTHrP antibody significantly inhibited Ca9-CM-induced *Rankl* expression in ST2 cells (Figure 5C). Interestingly, anti-mouse IL-6 receptor antibody inhibited *Rankl* mRNA expression more effectively than anti-human PTHrP antibody (Figure 5C). These results suggest that IL-6 synthesized not only by human oral cancer cells but also by mouse ST2 cells can stimulate *Rankl* expression in ST2 cells.

As shown in Figure 5D, antibodies against both human PTHrP and mouse IL-6 receptor significantly inhibited BHY-CM-induced osteoclast formation. Considered collectively, these results suggest that IL-6 and PTHrP are involved in the osteoclast formation induced by OSCC.

Oral Cancers Induce IL-6 Expression in Stromal Cells, Leading to RANKL Expression

The results described above suggest that oral cancer cells induce IL-6 expression in stromal cells and that this cytokine in turn plays a role in osteoclast formation induced by OSCC. The distribution of IL-6-positive fibroblastic cells in human gingival SCC as determined by immunohistochemical analysis (Figures 2 and 3) strongly supports this hypothesis. To confirm this finding, we investigated the effects of the CM derived from all of the
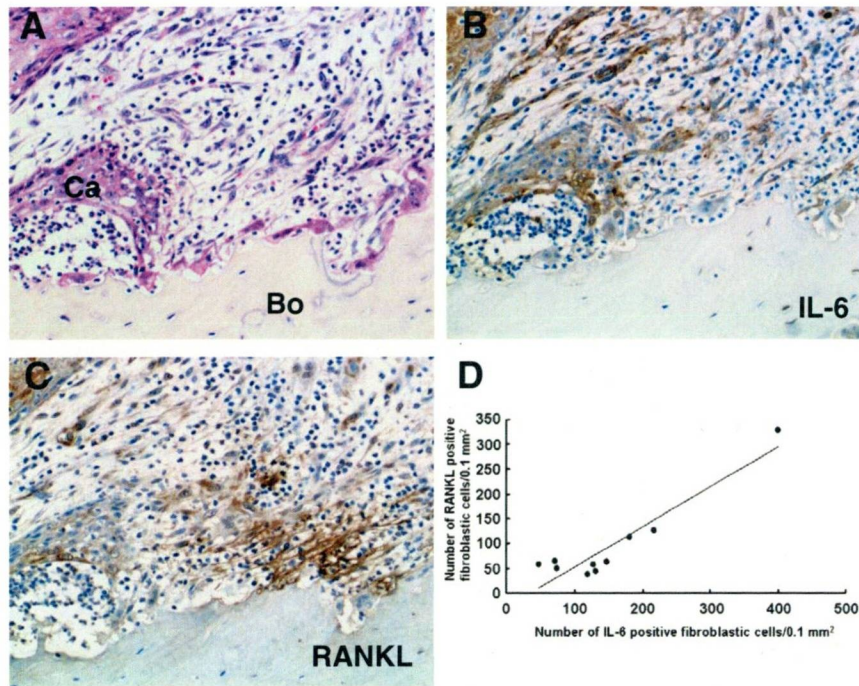
Figure 2. Distribution of RANKL-positive and IL-6-positive cells at the interface of the tumor front and resorbing bone in human gingival SCC. **A:** Histological analysis of tumor-bone interface. Ca, cancer cells; Bo, bone. H&E staining. **B:** Distribution of IL-6-positive cells. **C:** Distribution of RANKL-positive cells. Cells stained brown in **B** and **C** represent positive cells for each antibody. Original magnification, ×200. **D:** Correlation between the number of RANKL-positive and IL-6-positive fibroblastic cells at the tumor-bone interface in 10 human gingival SCCs; a positive correlation was noted ($r = 0.935926$, $Y = 0.8115X - 28.644$, $P < 0.0001$).

cancer cell lines on IL-6 expression in stromal cells. We found that CM derived from oral cancer cell lines significantly increased *Il-6* mRNA expression in ST2 cells (Figure 6A). The stimulatory effects of CM derived from BHY and HSC3 cells were much higher than those of CM from Ca9 and HO1 cells. The CM derived from the non-oral cancer cell lines, with the exception of MCF7, failed to induce *Il-6* mRNA expression (Figure 6A). The CM derived from every cancer cell line induced the production of IL-6 protein from ST2 cells in a similar fashion to levels
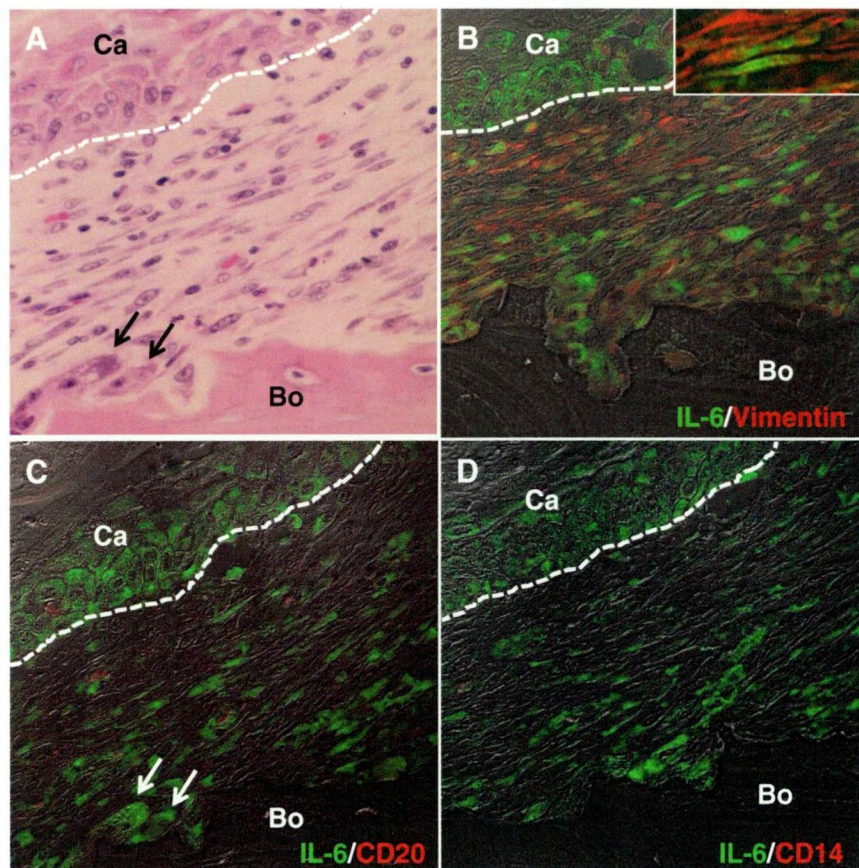

Figure 3. Characterization of IL-6-positive cells at the interface of the tumor front and resorbing bone in human gingival SCC. **A:** Histology of the tumor-bone interface. H&E staining. **B:** Dual immunohistochemical analysis for IL-6 (green) and vimentin (red). **Inset:** High magnification image of the fibroblastic cells dual positive for IL-6 and vimentin. **C:** Dual staining for IL-6 (green) and CD20 (red). **D:** Dual staining for IL-6 (green) and CD14 (red). **A** and **C** are the same section; the section was stained with H&E (**A**) after pictures were taken for immunohistochemical analysis in (**C**). **White dotted lines** indicate interfaces of cancer nest and stroma. **Arrows** in **A** and **C** indicate osteoclasts. Ca, cancer cells, Bo, Bone. Original magnification: ×400 (**A–D**); ×1600 (**inset in A**).
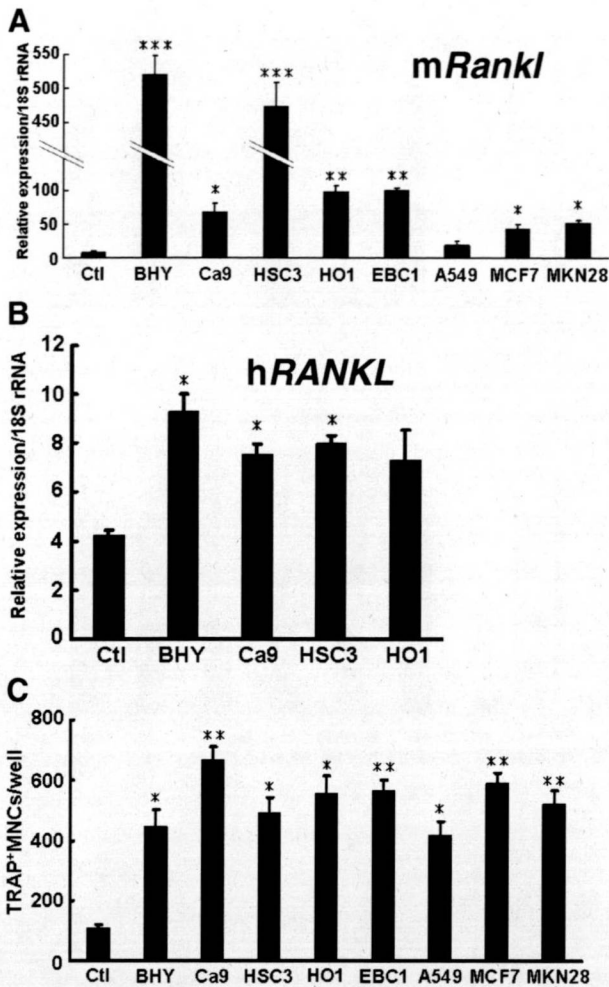
Figure 4. Effects of CM on *RANKL* expression in stromal cells and on osteoclast formation. Effects of CM derived from various cancer cell lines on mouse *Rankl* (m*Rankl*) mRNA expression in ST2 cells (**A**). ST2 cells were cultured for 2 days in the presence or absence (Ctl) of CM derived from various cancer cell lines, and the expression levels of *Rankl* were determined by using mouse specific primers. *$P < 0.05$, **$P < 0.01$, ***$P < 0.005$, significantly different from Ctl. **B:** Effects of CM derived from OSCC cell lines on human *RANKL* (h*RANKL*) mRNA expression in human mesenchymal stem cells. These cells were cultured for 2 days with or without (Ctl) CM, and the expression levels of *RANKL* were determined by using human specific primers. *$P < 0.01$, significantly different from Ctl. **C:** Effect of CM derived from various cancer cell lines on osteoclast formation. Osteoclast formation was assessed by adding CM from various cancer cell lines to coculture of ST2 with mouse bone marrow cells as described in *Materials and Methods*. *$P < 0.01$, **$P < 0.005$, significantly different from the control (Ctl). TRAP, tartrate-resistant acid phosphatase; MNCs, mononuclear cells.

of *Il-6* mRNA induced by each CM (Figure 6B). CM derived from OSCC cell lines also enhanced *IL-6* mRNA expression in human mesenchymal stem cells (Figure 6C). These results indicate that oral cancer cells effectively induce IL-6 expression in stromal cells. None of the CM induced *Pthrp* or *Tnf-α* mRNA expression in ST2 cells (Supplemental Figure S2, see *http://ajp.amjpathol.org*).

To discriminate between the roles of IL-6 synthesized by cancer cells and stromal cells in the induction of *Rankl* expression, we conducted experiments using antibodies that specifically neutralize human IL-6 and mouse IL-6. Both antibodies inhibited BHY-CM-induced *Rankl* mRNA expression in ST2 cells (Figure 7A). Moreover, compared with treatment with one of these antibodies alone, simul-
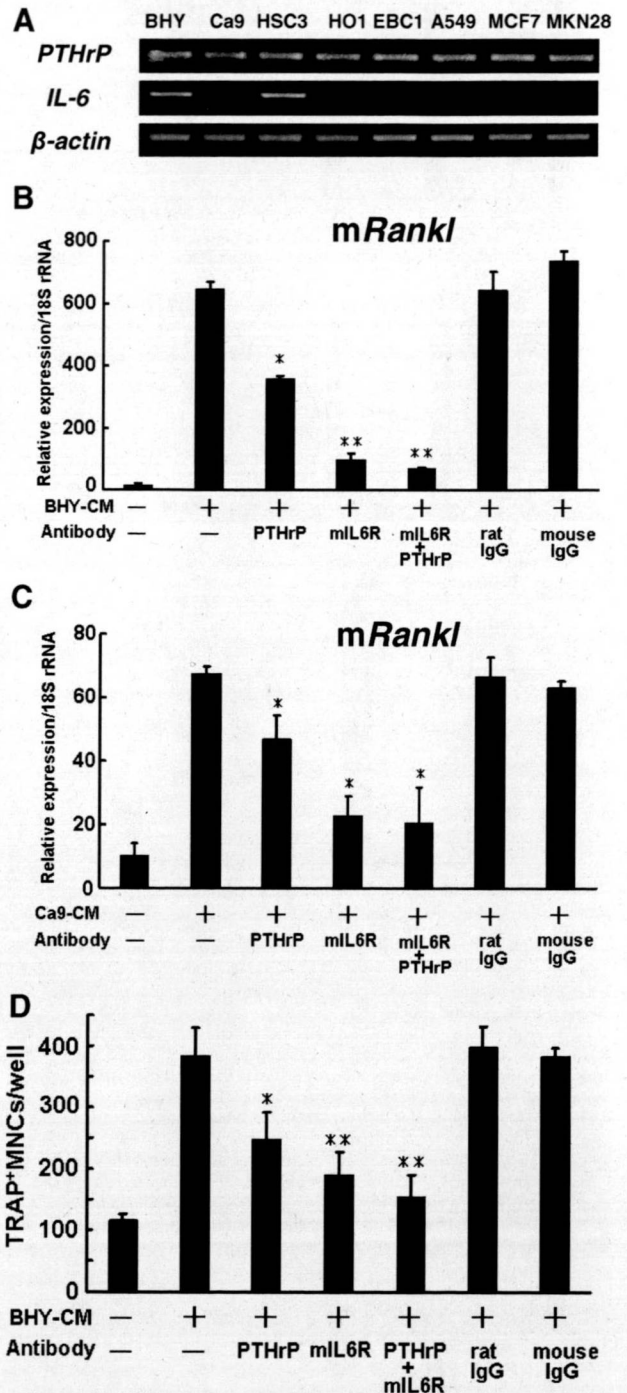

Figure 5. Role of IL-6 and PTHrP in *Rankl* expression and osteoclast formation. **A:** mRNA expression of *IL-6* and *PTHrP* in various cancer cell lines. **B** and **C:** Effects of anti-human PTHrP antibody and anti-mouse IL-6 (mIL-6) receptor antibody on *Rankl* mRNA expression induced by BHY-CM (**B**) and Ca9-CM (**C**) in ST2 cells. ST2 cells were cultured for 2 days in the presence or absence of BHY or Ca9-CM, and the expression of *Rankl* was determined by using mouse specific primers. *$P < 0.05$, **$P < 0.01$, significantly different from the value for BHY-CM(+) and antibody(−) in **B**, and *$P < 0.05$, significantly different from the value for Ca9-CM(+) and antibody (−) in **C**. **D:** Effects of anti-human PTHrP and anti-mouse IL-6 receptor antibodies on formation of tartrate-resistant acid phosphatase (TRAP)-positive osteoclast after stimulation with BHY-CM in cocultured ST2 and bone marrow cells. *$P < 0.01$, **$P < 0.005$, significantly different from the value of BHY-CM treated cells without any antibodies. In each experiment, the cells were treated with 10 μg/ml of each antibody. MNCs, multinucleated cells.
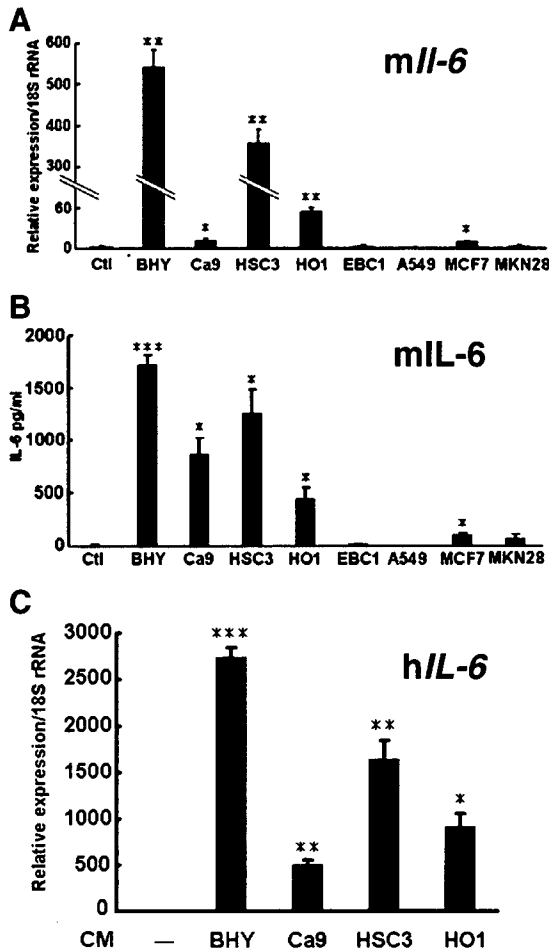
Figure 6. Stimulation of IL-6 in ST2 cells and human mesenchymal stem cells by various cancer cell lines. Effects of CM derived from various cancer cell lines on *Il-6* mRNA expression (A) and IL-6 production (B) in ST2 cells. ST2 cells were cultured for 2 days in the presence or absence (Ctl) of CM derived from various cancer cells and mouse *Il-6* (mIL-6) mRNA expression was determined by using mouse specific primers (A). IL-6 protein levels secreted by ST2 cells, which were measured by enzyme-linked immunosorbent assay using culture supernatants obtained from ST2 cells cultured for 24 hours with various CM in the absence of FBS (B). *P < 0.05, **P < 0.005, ***P < 0.0005, significantly different from the control culture (Ctl). C: Effects of CM derived from OSCC cell lines on human *IL-6* (hIL-6) mRNA expression in human mesenchymal stem cells. These cells were cultured for 2 days in the presence or absence of CM derived from OSCC cells, and the expression of human *IL-6* mRNA was examined by using human specific primers. *P < 0.001, **P < 0.005, ***P < 0.0005, significantly different from human mesenchymal stem cells cultured in the absence of any CM.

taneous treatment with both produced an additive inhibitory effect on *Rankl* mRNA expression (Figure 7A). When we used CM derived from Ca9 cells (Ca9-CM), which expressed *IL-6* mRNA at undetectable levels (Figure 5A), the anti-human IL-6 antibody did not alter *Rankl* mRNA expression, whereas anti-mouse IL-6 antibody significantly inhibited it (Figure 7B). These results demonstrate that IL-6 synthesized by both cancer cells and stromal cells induces RANKL expression in stromal cells.

We explored the factors that regulate IL-6 production in stromal cells. Because PTHrP is reported to stimulate IL-6 synthesis in osteoblastic cells,[37] we examined the effects of anti-human PTHrP antibody on *Il-6* mRNA expression in ST2 cells. As shown in Figure 7C, this antibody partially inhibited OSCC (BHY, Ca9, HSC3, and
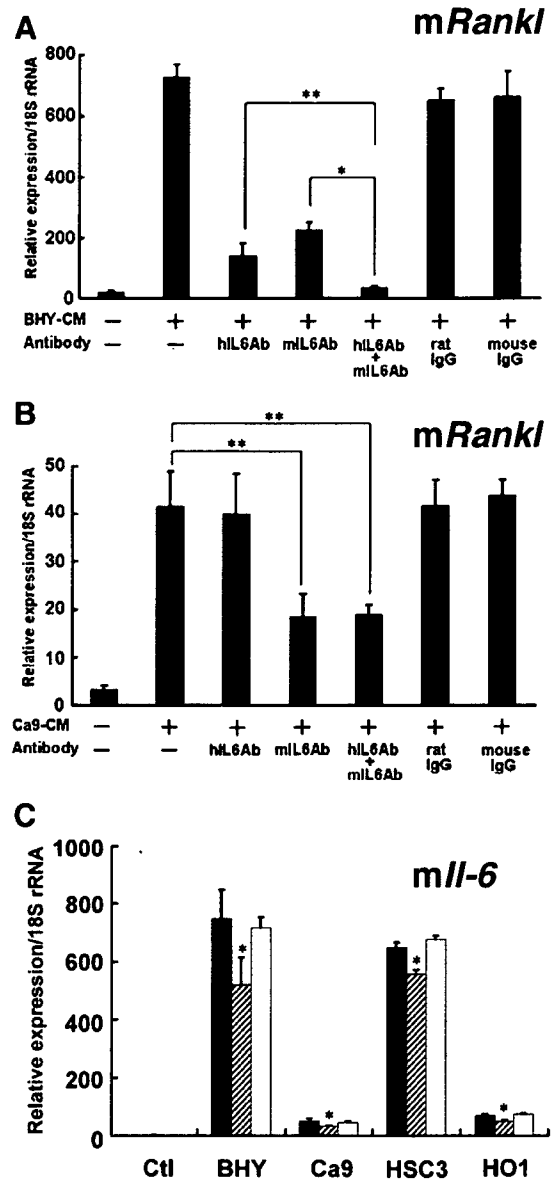

Figure 7. Effects of anti-human IL-6 antibody (hIL6Ab) and anti-mouse IL-6 antibody (mIL6Ab) on *Rankl* mRNA expression induced by BHY-CM (A) and Ca9-CM (B) in ST2 cells. ST2 cells were cultured for 2 days in the presence or absence of each CM, and the *Rankl* mRNA expression in ST2 cells was determined by using mouse specific primers. *P < 0.01, **P < 0.05. C: Effect of anti-human PTHrP antibody on mouse *Il-6* mRNA expression induced by CM-isolated from OSCC cell lines in ST2 cells. ST2 cells were cultured for 2 days in the presence or absence of CM isolated from each OSCC cell line, and the effect of anti-PTHrP antibody on *Il-6* expression was determined. In each experiment, the cells were treated with 10 μg/ml each antibody. Black bars, values treated with each CM only; gray bars, values treated with each CM and anti-PTHrP antibody; white bars, values treated with each CM and normal mouse IgG₁ (10 μg/ml). *P < 0.05, significantly different from each CM induced *Il-6* mRNA expression.

HO1)-induced *Il-6* mRNA expression (15 to 36% inhibition) at a concentration of 10 μg/ml. Almost the same inhibitory effects on BHY-CM-induced *Il-6* mRNA expression in ST2 cells occurred at concentrations of 5 and 10 μg/ml of anti-PTHrP antibody (Supplemental Figure S3, see *http://ajp.amjpathol.org*), suggesting that the concentration of anti-PTHrP antibody used (10 μg/ml) exerted the maximum inhibitory effect. These results support the
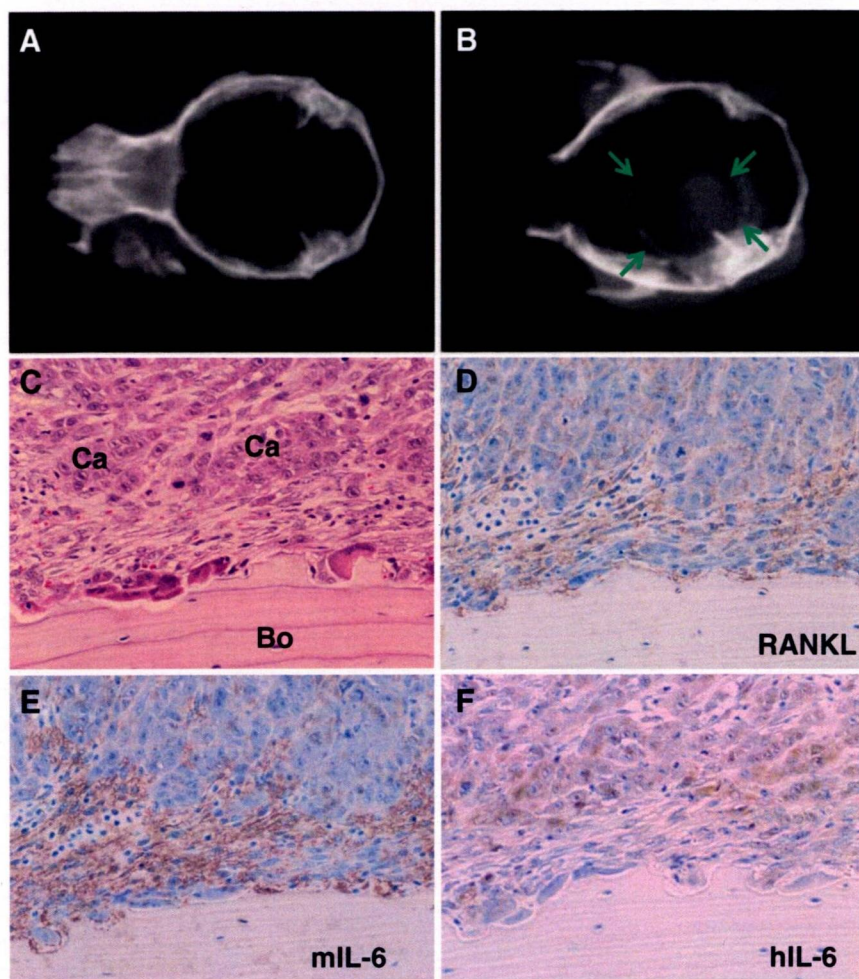
Figure 8. Xenograft experiments of HSC3 cells into athymic mice. The HSC3 cells were transplanted onto the periosteal region of parietal bone as described in *Materials and Methods.* **A** and **B:** Bone resorption was confirmed by soft X-ray examination 3 weeks after transplantation. A soft X-ray picture of calvaria in control group with injection of PBS only (**A**). A soft X-ray picture of calvaria in experimental group with injection of HSC3 cells (**B**). **Arrows** in **B** indicate the margin of bone destruction. **C–F:** Histology of bone resorbing region by HSC3 cells in semiserial sections. **C:** Typical histological appearance of the bone resorbing region by HSC3 cells. Note that fibroblastic cells are scattered between cancer cells (Ca) and bone (Bo) surface. Numerous osteoclasts are observed on the bone surface. H&E stain. **D:** Immunohistochemical analysis of RANKL. Note the RANKL-positive fibroblastic cells between cancer cells and bone surface. **E:** Immunohistochemical analysis of mouse IL-6 (mIL-6). Note that only fibroblastic cells between cancer cells and bone surface are positive for mIL-6. **F:** Immunohistochemical analysis of human IL-6 (hIL-6). Note that only cancer cells are positive for hIL-6.

hypothesis that PTHrP is partially involved in the regulation of cancer-induced IL-6 expression in stromal cells.

Xenograft Experiments of HCS3 Cells into Athymic Mice

Soft X-ray analysis revealed that transplantation of HSC3 cells onto the periosteal region of the parietal bone induced marked bone destruction in all athymic mice injected with HSC3 cells (*n* = 3) (Figure 8, A and B). Histologically, many osteoclasts were observed on the bone surface exposed to the injected cancer cells (Figure 8C). In addition, numerous fibroblastic cells were located between the cancer cells and the resorbing bone surface. These findings are similar to the bone resorption caused by human OSCC found in the surgical specimens. We therefore investigated the expression of RANKL, human IL-6, and mouse IL-6 by immunohistochemistry. The fibroblastic cells between the cancer cells and the bone surface expressed RANKL (Figure 8D). Interestingly, mouse IL-6 was identified in the fibroblastic cells (Figure 8E), which originated from athymic mice, whereas the expression of human IL-6 was limited to the cancer cells, which were derived from human OSCC (Figure 8F).

Discussion

Several reports have demonstrated that the elevated levels of serum IL-6 in patients with head and neck SCC serve as a valuable biomarker for predicting clinical outcome such as radioresistance, recurrence, and survival.[16–18] However, direct evidence of IL-6 production by OSCC is not well documented. Woods et al[38] reported that IL-6 was expressed in all of the 12 OSCC specimens examined, but other groups have reported that the expression levels varied among the OSCCs they tested.[17,39] The results of microarray analysis in the present study demonstrated that a few OSCC specimens expressed IL-6. Thus, the cells responsible for the elevated serum IL-6 levels noted in human OSCC patients should be investigated further. The immunohistochemical analysis in this study using bone-invasive human gingival SCC specimens revealed that IL-6 was expressed both in cancer cells located at the periphery of the cancer nests and in the fibroblastic cells at the tumor-bone interface. Because various cell types produce IL-6, we confirmed the nature of IL-6-producing cells by dual fluorescence immunohistochemistry and found that fibroblastic cells, not B cells or macrophages, are the major cells responsible for IL-6 production. Furthermore, the number of IL-6-positive fibroblastic cells significantly correlated with

the number of RANKL-positive fibroblastic cells at the tumor-bone interface. We also found that oral cancer cell lines effectively stimulated IL-6 synthesis in cultured stromal cells and that this cytokine participates in the induction of RANKL expression.

Thus, we are the first group to propose that IL-6 synthesized by stromal cells plays a significant role in OSCC-induced osteoclast formation, but the regulatory mechanism by which OSCC cells stimulate IL-6 synthesis in stromal cells remains unclear. We demonstrated that an anti-PTHrP antibody partially inhibited OSCC-CM-induced *Il-6* expression in ST2 cells. PTHrP is reported to induce IL-6 production in osteoblastic cells[37]; thus, it might be one of the secretions of OSCC that stimulates IL-6 expression in stromal cells. Mata et al[40] reported on the synergistic effects of IL-6 and PTHrP on bone resorption, and so PTHrP might enhance IL-6 activity during bone destruction by OSCC. However, other factors involved in induction of IL-6 in stromal cells should be explored because anti-PTHrP antibody exerted only partial inhibitory effects (15 to 36%) (Figure 7C). Sohara et al[41] reported that neuroblastoma cells also stimulate IL-6 production in bone marrow mesenchymal stem cells and that this cytokine subsequently activates osteoclasts. More recently, they demonstrated that galectin-3-binding protein secreted by neuroblastoma cells is responsible for inducing IL-6 expression in bone marrow stromal cells.[42] It has also been reported that myeloma cells up-regulate IL-6 in bone marrow stromal cells.[43,44] In the present study, we found that IL-6 expression in stromal cells was enhanced to a greater degree by CM derived from OSCC cells than by those derived from non-oral cancer cells, suggesting that the specific factor(s) produced by OSCC induces IL-6 expression in stromal cells.

We identified IL-6-positive osteoclasts on the resorbing bone surface at the tumor-bone interface by immunohistochemical analysis. Expression of IL-6 in osteoclasts has been reported in several bone diseases, such as Paget's disease of bone,[45] giant cell tumors,[46] renal osteodystrophy,[47] and fibrous dysplasia of bone.[48] It was suggested that the numbers of IL-6-expressing osteoclasts are significantly higher in osteoclasts within diseased bone than in normal osteoclasts.[48] Previous reports suggested that IL-6 synthesized by osteoclasts plays a role in osteoclastogenesis via an autocrine/paracrine fashion in pathological bone diseases.[46,49,50] Thus, IL-6 synthesized by stromal cells, cancer cells, and osteoclasts may collaborate to induce osteoclastic bone resorption in OSCC-associated bone destruction and elevate serum IL-6 levels in patients with OSCC.

In the present study, microarray analyses of human primary OSCC specimens revealed that many of the specimens overexpressed *PTHrP* mRNA. The *PTHrP* expression profile identified in this study was consistent with that described in previous reports.[26,27] By using a neutralizing antibody against PTHrP, we found that PTHrP is involved in *Rankl* mRNA expression in stromal cells and osteoclast formation induced by CM derived from oral cancer cells. These results provide the first evidence that PTHrP synthesized by oral cancer cells participates in osteoclast formation. Although these findings suggest that PTHrP is involved
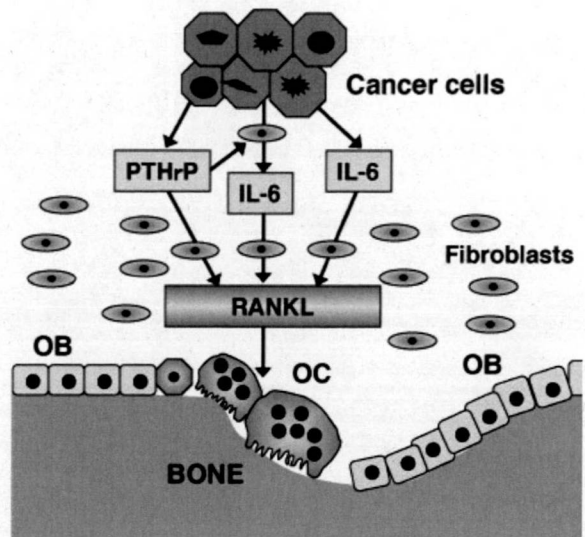

Figure 9. Schematic representation of the roles of IL-6 and PTHrP in OSCC-induced osteoclast formation. OC, osteoclasts; OB, osteoblasts.

in bone resorption induced by OSCC, the contribution of PTHrP to bone destruction might be smaller than that of IL-6 because neutralizing antibody against IL-6 more effectively inhibited *Rankl* expression in ST2 cells and osteoclast formation than that against PTHrP.

Figure 9 summarizes our hypothesis that IL-6 and PTHrP play important roles in OSCC-induced osteoclast formation. OSCC cells provide a suitable microenvironment for osteoclast formation not only by producing IL-6 and PTHrP but also by stimulating stromal cells to synthesize IL-6. IL-6 and PTHrP produced by OSCC cells and IL-6 by stromal cells induce fibroblastic cells/osteoblasts to synthesize RANKL, and subsequently they activate osteoclast formation and bone resorption. To prove this hypothesis, suitable *in vivo* experimental models are required. A few animal models have been generated for this purpose in previous studies[13,14]; however, in these models, OSCC cells are usually in direct contact with the resorbing bone surface lacking the substantial amount of fibrous stroma typically observed in the case of bone-invasive human OSCC. Therefore, these models will not be of much help in clarifying the role of IL-6 synthesized by stromal cells in response to OSCC. To overcome this problem, we successfully developed a suitable bone destruction model by xenotransplantation of OSCC cells (HSC3) into the periosteal region of athymic mice, which exhibits bone invasion patterns similar to those of human OSCC. In this model, we confirmed RANKL expression in fibroblastic cells at the tumor-bone interface. IL-6 expression was also identified in both fibroblastic and cancer cells. Thus, this model will be useful in understanding molecular mechanisms underlying cancer-associated bone destruction.

References

1. Semba I, Matsuuchi H, Miura Y: Histomorphometric analysis of osteoclastic resorption in bone directly invaded by gingival squamous cell carcinoma. J Oral Pathol Med 1996, 25:429–435
2. Wong RJ, Keel SB, Glynn RJ, Varvares MA: Histological pattern of mandibular invasion by oral squamous cell carcinoma. Laryngoscope 2000, 110:65–72
3. Brown JS, Lowe D, Kalavrezos N, D'Souza J, Magennis P, Woolgar J: Patterns of invasion and routes of tumor entry into the mandible by oral squamous cell carcinoma. Head Neck 2002, 24:370–383
4. Shaw RJ, Brown JS, Woolgar JA, Lowe D, Rogers SN, Vaughan ED: The influence of the pattern of mandibular invasion on recurrence and survival in oral squamous cell carcinoma. Head Neck 2004, 26:861–869
5. Takayanagi H: Osteoimmunology: shared mechanisms and crosstalk between the immune and bone systems. Nat Rev Immunol 2007, 7:292–304
6. Boyce BF, Xing L: Functions of RANKL/RANK/OPG in bone modeling and remodeling. Arch Biochem Biophys 2008, 473:139–146
7. Thomas GP, Baker SU, Eisman JA, Gardiner EM: Changing RANKL/OPG mRNA expression in differentiating murine primary osteoblasts. J Endocrinol 2001, 170:451–460
8. Lacey DL, Timms E, Tan HL, Kelley MJ, Dunstan CR, Burgess T, Elliott R, Colombero A, Elliott G, Scully S, Hsu H, Sullivan J, Hawkins N, Davy E, Capparelli C, Eli A, Qian YX, Kaufman S, Sarosi I, Shalhoub V, Senaldi G, Guo J, Delaney J, Boyle WJ: Osteoprotegerin ligand is a cytokine that regulates osteoclast differentiation and activation. Cell 1998, 93:165–176
9. Yasuda H, Shima N, Nakagawa N, Yamaguchi K, Kinosaki M, Mochizuki S, Tomoyasu A, Yano K, Goto M, Murakami A, Tsuda E, Morinaga T, Higashio K, Udagawa N, Takahashi N, Suda T: Osteoclast differentiation factor is a ligand for osteoprotegerin/osteoclastogenesis-inhibitory factor and is identical to TRANCE/RANKL. Proc Natl Acad Sci USA 1998, 95:3597–3602
10. Simonet WS, Lacey DL, Dunstan CR, Kelley M, Chang MS, Luthy R, Nguyen HQ, Wooden S, Bennett L, Boone T, Shimamoto G, DeRose M, Elliott R, Colombero A, Tan HL, Trail G, Sullivan J, Davy E, Bucay N, Renshaw-Gegg L, Hughes TM, Hill D, Pattison W, Campbell P, Sander S, Van G, Tarpley J, Derby P, Lee R, Boyle WJ: Osteoprotegerin: a novel secreted protein involved in the regulation of bone density. Cell 1997, 89:309–319
11. Okamoto M, Hiura K, Ohe G, Ohba Y, Terai K, Oshikawa T, Furuichi S, Nishikawa H, Moriyama K, Yoshida H, Sato M: Mechanism for bone invasion of oral cancer cells mediated by interleukin-6 in vitro and in vivo. Cancer 2000, 89:1966–1975
12. Tada T, Jimi E, Okamoto M, Ozeki S, Okabe K: Oral squamous cell carcinoma cells induce osteoclast differentiation by suppression of osteoprotegerin expression in osteoblasts. Int J Cancer 2005, 116:253–262
13. Shibahara T, Nomura T, Cui NH, Noma H: A study of osteoclast-related cytokines in mandibular invasion by squamous cell carcinoma. Int J Oral Maxillofac Surg 2005, 34:789–793
14. Cui N, Nomura T, Noma H, Yokoo K, Takagi R, Hashimoto S, Okamoto M, Sato M, Yu G, Guo C, Shibahala T: Effect of YM529 on a model of mandibular invasion by oral squamous cell carcinoma in mice. Clin Cancer Res 2005, 11:2713–2719
15. O'Brien CA, Gubrij I, Lin SC, Saylors RL, Manolagas SC: STAT3 activation in stromal/osteoblastic cells is required for induction of the receptor activator of NF-κB ligand and stimulation of osteoclastogenesis by gp130-utilizing cytokines or interleukin-1 but not 1,25-dihydroxyvitamin D_3 or parathyroid hormone. J Biol Chem 1999, 274:19301–19308
16. Jablonska E, Piotrowski L, Grabowska Z: Serum levels of IL-1β, IL-6, TNF-α, sTNF-RI and CRP in patients with oral cavity cancer. Pathol Oncol Res 1997, 3:126–129
17. Chen Z, Malhotra PS, Thomas GR, Ondrey FG, Duffey DC, Smith CW, Enamorado I, Yeh NT, Kroog GS, Rudy S, McCullagh L, Mousa S, Quezado M, Herscher LL, Van Waes C: Expression of proinflammatory and proangiogenic cytokines in patients with head and neck cancer. Clin Cancer Res 1999, 5:1369–1379
18. Duffy SA, Taylor JM, Terrell JE, Islam M, Li Y, Fowler KE, Wolf GT, Teknos TN: Interleukin-6 predicts recurrence and survival among head and neck cancer patients. Cancer 2008, 113:750–757
19. Burtis WJ, Wu T, Bunch C, Wysolmerski JJ, Insogna KL, Weir EC, Broadus AE, Stewart AF: Identification of a novel 17,000-dalton parathyroid hormone-like adenylate cyclase-stimulating protein from a tumor associated with humoral hypercalcemia of malignancy. J Biol Chem 1987, 262:7151–7156
20. Strewler GJ, Stern PH, Jacobs JW, Eveloff J, Klein RF, Leung SC, Rosenblatt M, Nissenson RA: Parathyroid hormonelike protein from human renal carcinoma cells. Structural and functional homology with parathyroid hormone, J Clin Invest 1987, 80:1803–1807
21. Moseley JM, Kubota M, Diefenbach-Jagger H, Wettenhall RE, Kemp BE, Suva LJ, Rodda CP, Ebeling PR, Hudson PJ, Zajac JD, Martin TJ: Parathyroid hormone-related protein purified from a human lung cancer cell line. Proc Natl Acad Sci USA 1987, 84:5048–5052
22. Shulkes A, Fletcher DR, Rubinstein C, Ebeling PR, Martin TJ: Production of calcitonin gene related peptide, calcitonin and PTH-related protein by a prostatic adenocarcinoma. Clin Endocrinol (Oxf) 1991, 34:387–393
23. Malakouti S, Asadi FK, Kukreja SC, Abcarian HA, Cintron JR: Parathyroid hormone-related protein expression in the human colon: immunohistochemical evaluation. Am Surg 1996, 62:540–544; discussion 544–545
24. Dunne FP, Bowden SJ, Brown JS, Ratcliffe WA, Browne RM: Parathyroid hormone related protein in oral squamous cell carcinomas invading the mandible. J Clin Pathol 1995, 48:300–303
25. Tsuchimochi M, Kameta A, Sue M, Katagiri M: Immunohistochemical localization of parathyroid hormone-related protein (PTHrP) and serum PTHrP in normocalcemic patients with oral squamous cell carcinoma. Odontology 2005, 93:61–71
26. Kornberg LJ, Villaret D, Popp M, Lui L, McLaren R, Brown H, Cohen D, Yun J, McFadden M: Gene expression profiling in squamous cell carcinoma of the oral cavity shows abnormalities in several signaling pathways. Laryngoscope 2005, 115:690–698
27. Deyama Y, Tei K, Yoshimura Y, Izumiyama Y, Takeyama S, Hatta M, Totsuka Y, Suzuki K: Oral squamous cell carcinomas stimulate osteoclast differentiation. Oncol Rep 2008, 20:663–668
28. Roodman GD: Biology of osteoclast activation in cancer. J Clin Oncol 2001, 19:3562–3571
29. Karnoub AE, Dash AB, Vo AP, Sullivan A, Brooks MW, Bell GW, Richardson AL, Polyak K, Tubo R, Weinberg RA: Mesenchymal stem cells within tumour stroma promote breast cancer metastasis. Nature 2007, 449:557–563
30. Mishra PJ, Mishra PJ, Glod JW, Banerjee D: Mesenchymal stem cells: flip side of the coin. Cancer Res 2009, 69:1255–1258
31. Ishikuro M, Sakamoto K, Kayamori K, Akashi T, Kanda H, Izumo T, Yamaguchi A: Significance of the fibrous stroma in bone invasion by human gingival squamous cell carcinomas. Bone 2008, 43:621–627
32. Takagi N, Mihara M, Moriya Y, Nishimoto N, Yoshizaki K, Kishimoto T, Takeda Y, Ohsugi Y: Blockage of interleukin-6 receptor ameliorates joint disease in murine collagen-induced arthritis. Arthritis Rheum 1998, 41:2117–2121
33. Onuma E, Sato K, Saito H, Tsunenari T, Ishii K, Esaki K, Yabuta N, Wakahara Y, Yamada-Okabe H, Ogata E: Generation of a humanized monoclonal antibody against human parathyroid hormone-related protein and its efficacy against humoral hypercalcemia of malignancy. Anticancer Res 2004, 24:2665–2673
34. Nguyen ST, Hasegawa S, Tsuda H, Tomioka H, Ushijima M, Noda M, Omura K, Miki Y: Identification of a predictive gene expression signature of cervical lymph node metastasis in oral squamous cell carcinoma. Cancer Sci 2007, 98:740–746
35. Tsutsumi S, Shimazu A, Miyazaki K, Pan H, Koike C, Yoshida E, Takagishi K, Kato Y: Retention of multilineage differentiation potential of mesenchymal cells during proliferation in response to FGF. Biochem Biophys Res Commun 2001, 288:413–419
36. Kondo T, Kitazawa R, Yamaguchi A, Kitazawa S: Dexamethasone promotes osteoclastogenesis by inhibiting osteoprotegerin through multiple levels. J Cell Biochem 2008, 103:335–345
37. Guillén C, Martinez P, de Gortazar AR, Martinez ME, Esbrit P: Both N- and C-terminal domains of parathyroid hormone-related protein increase interleukin-6 by nuclear factor-kappa B activation in osteoblastic cells. J Biol Chem 2002, 277:28109–28117
38. Woods KV, El-Naggar A, Clayman GL, Grimm EA: Variable expression of cytokines in human head and neck squamous cell carcinoma cell lines and consistent expression in surgical specimens. Cancer Res 1998, 58:3132–3141
39. Wang YF, Chang SY, Tai SK, Li WY, Wang LS: Clinical significance of interleukin-6 and interleukin-6 receptor expressions in oral squamous cell carcinoma. Head Neck 2002, 24:850–858

40. de la Mata J, Uy HL, Guise TA, Story B, Boyce BF, Mundy GR, Roodman GD: Interleukin-6 enhances hypercalcemia and bone resorption mediated by parathyroid hormone-related protein in vivo. J Clin Invest 1995, 95:2846–2852

41. Sohara Y, Shimada H, Minkin C, Erdreich-Epstein A, Nolta JA, DeClerck YA: Bone marrow mesenchymal stem cells provide an alternate pathway of osteoclast activation and bone destruction by cancer cells. Cancer Res 2005, 65:1129–1135

42. Fukaya Y, Shimada H, Wang LC, Zandi E, DeClerck YA: Identification of galectin-3-binding protein as a factor secreted by tumor cells that stimulates interleukin-6 expression in the bone marrow stroma. J Biol Chem 2008, 283:18573–18581

43. Gunn WG, Conley A, Deininger L, Olson SD, Prockop DJ, Gregory CA: A crosstalk between myeloma cells and marrow stromal cells stimulates production of DKK1 and interleukin-6: a potential role in the development of lytic bone disease and tumor progression in multiple myeloma. Stem Cells 2006, 24:986–991

44. Arnulf B, Lecourt S, Soulier J, Ternaux B, Lacassagne MN, Crinquette A, Dessoly J, Sciaini AK, Benbunan M, Chomienne C, Fermand JP, Marolleau JP, Larghero J: Phenotypic and functional characterization of bone marrow mesenchymal stem cells derived from patients with multiple myeloma. Leukemia 2007, 21:158–163

45. Roodman GD, Kurihara N, Ohsaki Y, Kukita A, Hosking D, Demulder A, Smith JF, Singer FR: Interleukin 6. A potential autocrine/paracrine factor in Paget's disease of bone, J Clin Invest 1992, 89:46–52

46. Reddy SV, Takahashi S, Dallas M, Williams RE, Neckers L, Roodman GD: Interleukin-6 antisense deoxyoligonucleotides inhibit bone resorption by giant cells from human giant cell tumors of bone. J Bone Miner Res 1994, 9:753–757

47. Langub MC Jr, Koszewski NJ, Turner HV, Monier-Faugere MC, Geng Z, Malluche HH: Bone resorption and mRNA expression of IL-6 and IL-6 receptor in patients with renal osteodystrophy. Kidney Int 1996, 50:515–520

48. Riminucci M, Kuznetsov SA, Cherman N, Corsi A, Bianco P, Gehron Robey P: Osteoclastogenesis in fibrous dysplasia of bone: in situ and in vitro analysis of IL-6 expression. Bone 2003, 33:434–442

49. Roodman GD: Regulation of osteoclast differentiation. Ann NY Acad Sci 2006, 1068:100–109

50. O'Keefe RA, Teot LA, Singh D, Puzas JE, Rosier RN, Hicks DG: Osteoclasts constitutively express regulators of bone resorption: an immunohistochemical and in situ hybridization study. Lab Invest 1997, 76:457–465

Latexin is involved in bone morphogenetic protein-2-induced chondrocyte differentiation

Ichiro Kadouchi [a,b], Kei Sakamoto [b], Liu Tangjiao [b,c], Takashi Murakami [d], Eiji Kobayashi [d], Yuichi Hoshino [a], Akira Yamaguchi [b,e,*]

[a] Department of Orthopedic Surgery, Jichi Medical University, Shimotsuke, Tochigi, Japan
[b] Section of Oral Pathology, Department of Oral Restitution, Graduate School of Tokyo Medical and Dental University, Bunkyo-ku, Tokyo 113-8549, Japan
[c] Section of Oral Pathology, College of Stomatology, Dalian Medical University, Dalian, China
[d] Division of Organ Replacement Research, Center for Molecular Medicine, Jichi Medical University, Shimotsuke, Tochigi, Japan
[e] Global Center of Excellence Program, International Research Center for Molecular Science in Tooth and Bone Diseases, Graduate School of Tokyo Medical and Dental University, Bunkyo-ku, Tokyo 113-8549, Japan

ARTICLE INFO

ABSTRACT

Latexin is the only known carboxypeptidase A inhibitor in mammals. We previously demonstrated that BMP-2 significantly induced *latexin* expression in Runx2-deficient mesenchymal cells (RD-C6 cells), during chondrocyte and osteoblast differentiation. In this study, we investigated latexin expression in the skeleton and its role in chondrocyte differentiation. Immunohistochemical studies revealed that proliferating and prehypertrophic chondrocytes expressed latexin during skeletogenesis and bone fracture repair. In the early phase of bone fracture, *latexin* mRNA expression was dramatically upregulated. BMP-2 upregulated the expression of the mRNAs of *latexin*, *Col2a1*, and the gene encoding aggrecan (*Agc1*) in a micromass culture of C3H10T1/2 cells. Overexpression of *latexin* additively stimulated the BMP-2-induced expression of the mRNAs of *Col2a*, *Agc1*, and *Col10a1*. BMP-2 treatment upregulated *Sox9* expression, and *Sox9* stimulated the promoter activity of *latexin*. These results indicate that latexin is involved in BMP-2-induced chondrocyte differentiation and plays an important role in skeletogenesis and skeletal regeneration.

© 2008 Elsevier Inc. All rights reserved.

Chondrocytes and osteoblasts originate from common progenitors called mesenchymal stem cells [1]. During the differentiation of these cells, bone morphogenetic proteins (BMPs) play a crucial role in inducing the expression of lineage-specific transcription factors such as Runx2 [1–3] and Sox9 [4,5]; Runx2 is an essential transcription factor that regulates osteoblast differentiation [1,6,7] and chondrocyte maturation [8], and Sox9 is an important transcription factor that regulates chondrocyte differentiation from mesenchymal stem cells [5,9].

We established a clonal cell line, RD-C6, from *Runx2*-deficient mouse embryos and demonstrated that this cell line could differentiate into both osteoblasts and chondrocytes in response to BMP-2 treatment via a Runx2-independent pathway [10]. By microarray analysis of this cell line with and without BMP-2 treatment, we identified latexin as a downstream factor of BMP-2 signaling [10]. This implied that latexin expression was regulated by BMP-2 signaling via a Runx2-independent pathway.

Latexin is composed of 222 amino acids and has a molecular weight of 29 kDa; further, it is the only known carboxypeptidase A inhibitor in mammals [11,12]. The latexin was discovered in the lateral neocortex of rats, and it acts as a marker of regionality and development of both the central and the peripheral nervous systems [11]. Further, *latexin* is expressed in several other tissues, including hematopoietic and lymphoid organs, and plays an important role in regulating the activity of hematopoietic stem cells [12,13]. By microarray analysis, Balint et al. [14] briefly mentioned that *latexin* was one of the upregulated genes in BMP-2-treated C2C12 cells. This suggests a possible role of latexin in osteoblast differentiation, because C2C12 cells exclusively differentiated into osteoblasts and not into chondrocytes by BMP-2 treatment [15]. In addition, we demonstrated that BMP-2 induced RD-C6 cells to differentiate into both osteoblast and chondrocyte lineage cells [10]. However, it remained unclear whether latexin is involved in osteogenic differentiation, chondrogenic differentiation, or both.

To investigate the role of latexin in skeletal cell differentiation, we first investigated latexin expression during skeletogenesis and skeletal regeneration and examined its role in chondrocyte differentiation by using a multipotent mesenchymal cell line, C3H10T1/2. Here, we describe that latexin is expressed in chondrocytes and involved in BMP-2-induced chondrocyte differentiation.

Materials and methods

Immunohistochemistry. Immunohistochemical staining was performed on 4% paraformaldehyde-fixed, ethylenediaminetetraacetic acid (EDTA)-decalcified, and paraffin-embedded sections. Endogenous peroxidase activity was blocked with 10% hydrogen peroxidase/methanol, and nonspecific binding was blocked with 10% horse serum. The sections were incubated with goat anti-latexin (Everest Biotech, Oxfordshire, UK) or rabbit anti-Sox9 (Santa Cruz Biotechnology Inc., Santa Cruz, CA) overnight at 4 °C. After washing, they were incubated with horseradish peroxidase-conjugated secondary antibodies (Dako, Glostrup, Denmark). The antigen-bound peroxidase activity was visualized by staining the sections with 3-amino-9-ethyl-carbazole (AEC) chromogen.

Fracture model. The midshafts of the tibiae of 8-week-old mice were fractured using a bone saw and internally stabilized with an intramedullary nail by using the inner pin of a spinal needle with 22-G diameter. The mice were sacrificed and submitted for histological and real-time reverse-transcriptase polymerase chain reaction (RT-PCR) analyses on 5, 10, and 15 days after the operation. All animal studies were approved by the Animal Ethics Committee of Jichi Medical University and performed in accordance with the Jichi Medical University Guide for the Care and Use of Laboratory Animals, following the principles of laboratory animal care formulated by the National Society for Medical Research.

Cell culture. C3H10T1/2 (clone 8) cells were purchased from Cell Bank, RIKEN BioResource Center (Tsukuba, Japan). The cells were maintained in Eagle's basal medium containing 10% fetal bovine serum (FBS; Sigma, St. Louis, MO), l-glutamine, 50 U/ml penicillin G, and 50 mg/ml streptomycin. For a micromass culture, the C3H10T1/2 cells were suspended in the medium at a concentration of 1×10^7 cells/ml, and a 10-μl drop of this cell suspension was placed in the center of a culture dish. The cells were allowed to adhere for 3 h, and a medium with or without recombinant human BMP-2 (rhBMP-2; 100 ng/ml; Astellas Pharma Inc., Tokyo, Japan) was added to the culture. The cells were stained with Alcian blue solution (pH 2.5) on days 2 and 4 *in vitro.*

Mouse cDNA containing *latexin* open reading frame was obtained by PCR and subcloned into pMSCV (Clontech, CA). Retrovirus was produced and cells were infected with the retrovirus according to the manufacturer's instructions. After infection, the cells were selected in a puromycin-containing medium for 2 weeks.

Western blot analysis. The cells were lysed with radioimmuno-precipitation assay (RIPA) buffer containing protease inhibitor cocktail (Roche Diagnostics, Basel, Switzerland). Western blot analysis was performed according to the standard procedure. SDS–polyacrylamide gel electrophoresis (PAGE) was performed using $1\times$ sample buffer containing 5% β-mercaptoethanol. The proteins were transferred to nitrocellulose membranes, which were then incubated with the following primary antibodies for 1 h: goat anti-latexin, rabbit anti-Sox9, and anti-actin (SC-1616; Santa Cruz Biotechnology Inc.). Next, the membranes were incubated with the respective secondary antibodies for 1 h. Chemiluminescence was detected with an enhanced chemiluminescence (ECL) Plus chemiluminescence detection kit (GE Healthcare, UK).

Real-time RT-PCR. Total RNA was extracted from the cultured cells using RNA Smart Total RNA Isolation Kit (Macherey-Nagel GmbH & Co. KG, Düren, Germany). RNA aliquots of 500 ng were reverse transcribed to cDNA by using a First-Strand cDNA synthesis kit for RT-PCR (Invitrogen Corp., Carlsbad, CA) and an oligo-dT primer. mRNA expression was quantified by real-time RT-PCR, using a MiniOpticon system (Bio-Rad Laboratories, Hercules, CA) with the iQ SYBR Green supermix (Bio-Rad Laboratories). Relative amount of each mRNA was normalized to 18 S rRNA expression. The primer sequences are listed in Table 1.

Table 1
Primers used for real-time-based RT-PCR.

	Forward primer	Reverse primer
Lxn	5′- GTCGCCTGCGGTTATGTAAT	5′- GGCGGCTGTTGTGTTTTACT
Col2a1	5′-TGCACGAAACACACTGGTAAG	5′- CACCAAATTCCTGTTCAGCC
Agc1	5′- AGGAGACCCAGACAGCAGAA	5′-ACAGTGACCCTGGAACTTGG
Col10a1	5′-TGGGTAGGCCTGTATAAAGAACGG	5′-CATGGGAGCCACTAGGAATCC TGAGA
Sox9	5′- CTCGCAATACGACTACGCT	5′-CTGGTTGTTCCCAGTGCT
18S rRNA	5′-GTAACCCGTTGAACCCCATT	5′-CCATCCAATCGGTAGTAGCG

Luciferase activity assay. The proximal promoter region of human *latexin* was obtained from a bacterial artificial chromosome (BAC) clone, RP11-bA39F4, by PCR, and the product was cloned into pGL3-basic (latexin-luc; Promega, Madison, WI). The latexin-luc plasmid was transfected into C3H10T1/2 cells, using Lipofectamine 2000 (Invitrogen) according to the manufacturer's instructions. The amount of latexin-luc plasmid was 0.5 μg in every experiment. Luciferase activity was measured 48 hours after the transfection by using a luciferase assay kit (Promega) according to the manufacturer's instructions.

Statistics. Statistical analyses were performed using Student's unpaired t-test. Each experiment was conducted at least twice. The data presented represent means ± standard deviation (SD) of independent replicates ($n > 3$).

Results

Some chondrocytes express latexin in embryonic skeleton and regenerative bone

We first investigated latexin expression during skeletogenesis in embryonic mice and skeletal regeneration in adult mice by immunohistochemistry. Latexin expression was observed in resting to prehypertrophic chondrocytes but not in hypertrophic chondrocytes in E15.5 embryos (Fig. 1A and B). The distribution of latexin-positive cells was similar to that of Sox9-positive cells (Fig. 1C and D). Some osteoblastic cells at periosteoal region in bone collar showed weak signals for latexin expression (Fig. 1A). The peripheral nerves at perichondral membrane exhibited strong signals of latexin (Fig. 1A).

We next examined latexin expression during bone fracture healing at the tibial diaphyses by immunohistochemistry (Fig. 1E–J). In our experimental model, chondrocytes appeared at the periosteal region around the bone fracture site on day 5 after the injury (Fig. 1E). Immunohistochemical studies revealed that many of these chondrocytes were positive for latexin (Fig. 1F). Interestingly, immunoreactivity was detected in the nuclei as well as the cytoplasm of numerous chondrocytes. Numerous hypertrophic chondrocytes and newly formed trabecular bones were observed on day 10, but only proliferating or prehypertrophic chondrocytes were positive for latexin (Fig. 1G and H). Hypertrophic chondrocytes showed no apparent signals for latexin expression (Fig. 1H). On day 15, the process of new bone formation progressed by replacing the pre-existing cartilage (Fig. 1I), and osteoblasts covering newly formed bone trabeculae showed no apparent signals of latexin (Fig. 1J). The number of latexin-positive cells dramatically decreased on day 15 as compared with those on days 5 and 10. No apparent signals were found in the osteoblastic cells covering the trabecular and cortical bones away from fracture sites.

Real-time RT-PCR analysis confirmed that *latexin* expression was undetectable before the injury; however, its expression dramatically increased on day 5 after the injury and then gradually declined on days 10 and 15 (Fig. 1K).

These results indicate that latexin is expressed in chondrogenic cells during skeletogenesis in mouse embryos, and its expression is
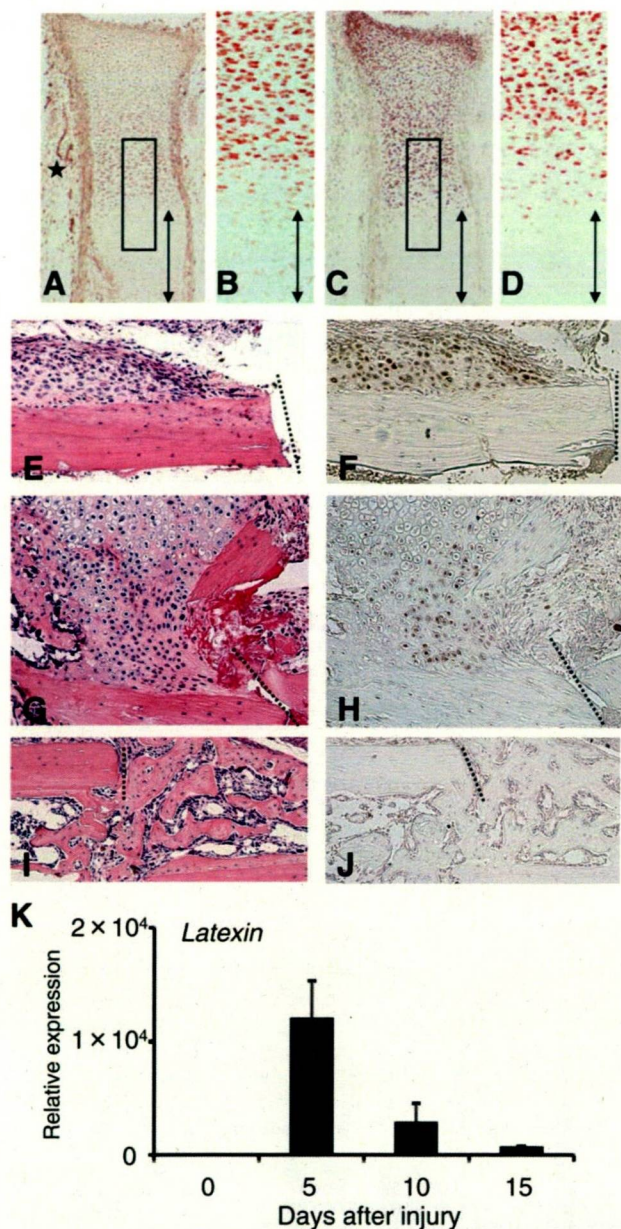
Fig. 1. Chondrocytes express latexin expression in the embryonic tibiae (A,B) and during skeletal regeneration in adult mice (F, H, and J). (A,B) Immunohistochemical staining of latexin in the tibia of an E15.5 mouse embryo. A higher magnification image of the square in A is shown in B. (C,D) Immunohistochemical staining of Sox9 in the tibia of an E15.5 mouse embryo. A higher magnification image of the square in C is shown in D. Arrows in A, B, C, and D indicate hypertrophic chondrocytes zones. An asterisk in A shows latexin-positive peripheral nerves. (E, G, and I) Hematoxylin–eosin staining images of fracture repair on days 5 (E), 10 (G) and 15 (I) after injury in tibiae of adult mice. (F, H, and J) Immunohistochemical staining of latexin during fracture repair. Note that latexin-positive chondrocytes in F and H. Hypertrophic chondrocytes in H and osteoblasts covering newly formed bone trabeculae exhibit few signals for latexin. Dotted lines in E–J indicate fracture end of cortical bones. (K) Latexin mRNA expression during fracture repair assessed by real-time RT-PCR as described in Materials and methods.

limited to the chondrocytes appearing during fracture repair in adult mice.

BMP-2 induces latexin expression in C3H10T1/2 cells along with chondrocyte differentiation

To investigate the role of latexin in chondrocyte differentiation, we used a micromass culture of C3H10T1/2 cells. The cultured cells produced Alcian blue-positive extracellular matrix on day 2, the amount of which increased on day 4 in the culture (Fig. 2A). BMP-2 treatment increased the production of Alcian blue-positive extracellular matrix on days 2 and 4 as compared with the respective control cultures (Fig. 2A). The treatment significantly increased the in vitro expression of the mRNA for Col2a1 and aggrecan (Agc1), which encode the major components of extracellular matrices synthesized by chondrocytes, on days 2 and 4 (Fig. 2B). These results indicate that C3H10T1/2 cells maintained in a micromass culture differentiate into chondrogenic cells in response to BMP-2. We next investigated latexin expression in C3H10T1/2 cells cultured in this system by real-time RT-PCR and Western blot analysis. BMP-2 upregulated the latexin expression on days 2 and 4 at the mRNA and protein levels (Fig. 2C and D). These results suggest that BMP-2 induces latexin expression along with chondrocyte differentiation.

Overexpression of latexin stimulates BMP-2-induced chondrocyte differentiation

We overexpressed mouse latexin gene in C3H10T1/2 cells by infecting the cells with a retrovirus. The infected cells were cultured with and without rhBMP-2 for 2 days. The cells overexpressing latexin induced no changes in the expression of the mRNAs of Col2a1, Agc1, and Col10a1 in the absence of BMP-2, compared with the control culture (Fig. 3). In contrast, the cells overexpressing latexin significantly increased the expression of the abovementioned mRNAs in the presence of BMP-2, as compared with the BMP-2-treated cells transduced with green fluorescent protein (GFP) (Fig. 3). These results suggest that latexin additively stimulates BMP-2-induced chondrocyte differentiation.

Sox9 stimulates the promoter activity of latexin

BMP-2 induced latexin expression in RD-C6 cells, Runx2-deficient cell line, as well as in C3H10T1/2 cells. These results prompted us to investigate whether BMP-2 directly stimulated the promoter activity of latexin, and we found that BMP-2 treatment induced no apparent stimulation of the promoter activity of latexin at concentrations of 100 and 500 ng/ml (data not shown). It has been reported that BMP-2 efficiently induces Sox9 expression along with chondrogenic differentiation [4,5], and we also confirmed BMP-2-induced upregulation of Sox9 mRNA expression in C3H10T1/2 cells on day 2 (Fig. 4A). Therefore, we investigated whether Sox9 regulates the promoter activity of latexin. As shown in Fig. 4B, Sox9 stimulated the promoter activity of latexin. These findings suggest that BMP-2-induced Sox9 regulates latexin expression in chondrogenic differentiation.

Discussion

Latexin is expressed in various tissues, including brain tissues and hematopoietic and lymphoid organs [11–13,16,17], but its expression and function in skeletal tissues have not been reported in detail. We previously identified latexin as a downstream factor of BMP signaling by a microarray analysis of RD-C6 cells, a Runx2-deficient cell line, with and without BMP-2 treatment [10]. Since BMP-2 treatment induced RD-C6 cells to differentiate into both osteoblasts and chondrocytes [10], we first investigated latexin expression during skeletogenesis and skeletal regeneration to identify the skeletal cells that express latexin in vivo by immunohistochemistry. This study revealed that the proliferating and prehypertrophic chondrocytes in the embryonic tibiae and callus appearing during skeletal regeneration in adult mice expressed latexin. Real-time RT-PCR analysis also indicated the great induction
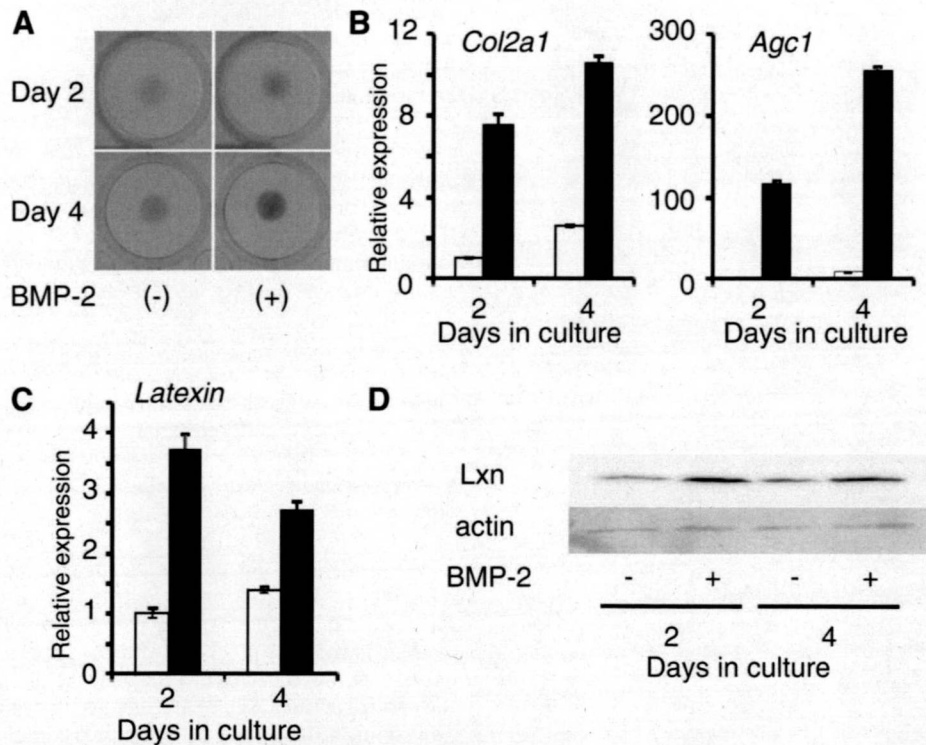
Fig. 2. BMP-2 stimulated the expression of *latexin* mRNA in a micromass culture of C3H10T1/2 cells along with chondrocyte differentiation. (A) Alcian blue staining of C3H10T1/2 cells cultured with and without BMP-2 (100 ng/ml) for 2 and 4 days. (B) Effects of BMP-2 on mRNA expression for *Col2a1* and *Agc1*. C3H10T1/2 cells were cultured for 2 and 4 days in the absence (open bars) and presence (closed bars) of BMP-2, and the expression of the abovementioned mRNAs was determined by real-time RT-PCR. (C) Effects of BMP-2 on the expression of *latexin* mRNA. C3H10T1/2 cells were cultured for 2 and 4 days in the absence (open bars) and presence (closed bars) of BMP-2. (D) Effects of BMP-2 on latexin expression. C3H10T1/2 cells were cultured for 2 and 4 days in the absence and presence of BMP-2, and latexin expression was examined by Western blot analysis as described in Materials and methods.
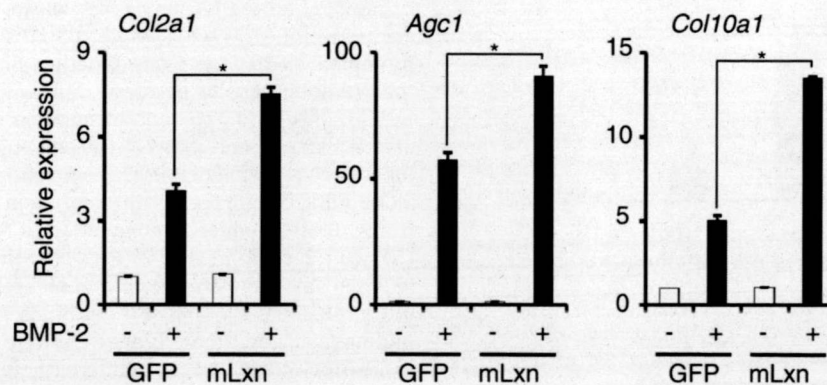

Fig. 3. Overexpression of latexin stimulated BMP-2-induced chondrocyte differentiation in a micromass culture of C3H10T1/2 cells. The cells were cultured for 2 days with and without BMP-2 (100 ng/ml). The expression of the mRNAs of *Col2a*, *Agc1*, and *Col10a1* were determined by real-time RT-PCR as described in Materials and methods). Relative amount of each mRNA was normalized to 18S rRNA expression. $^*P < 0.05$ versus control cells.

of *latexin* mRNA expression in the early phase of skeletal regeneration. Taken together, these results suggest that latexin plays an important role in skeletogenesis and skeletal regeneration.

These immunohistochemical findings prompted us to investigate the role of latexin in chondrocyte differentiation, for which we used a micromass culture of C3H10T1/2 cells. The culture experiments revealed that the expression of *latexin* mRNA correlated with that of other chondrocyte differentiation-related mRNAs such as those of *Col2a1* and *Agc1*. In addition, overexpression of *latexin* additively stimulated BMP-2-induced chondrocyte differentiation. Interestingly, overexpression of latexin induced no significant changes in the expression of the abovementioned mRNAs in the absence of BMP-2, suggesting a close interaction between the

regulation of *latexin* expression and BMP signaling. To further investigate the underlying mechanism, we examined the effects of BMP-2 on the activation of *latexin* promoter and found that BMP-2 did not stimulate the promoter. Since it has been reported that BMP-2 induces Sox9 expression [4,5], we examined the effects of *Sox9* on the transactivation of *latexin* promoter and demonstrated that *Sox9* stimulated the promoter activity of *latexin*. These results suggest that latexin is involved in chondrocyte differentiation via Sox9, the expression of which is upregulated by BMP-2. There have been no reports about the regulatory mechanism of *latexin* expression even in neural tissues, and *Sox9* is the first candidate transcription factor that regulates *latexin* expression. However, its *latexin*-transducing activity was not observed to be
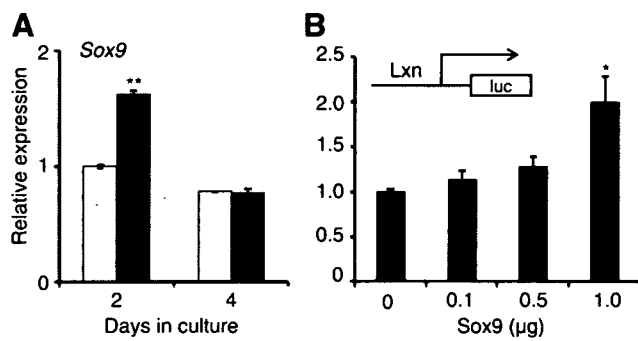
Fig. 4. BMP-2 induced the expression of *Sox9* mRNA in C3H10T1/2 cells, and Sox9 activated the promoter activity of *latexin*. (A) Effects of BMP-2 on the expression of *Sox9* mRNA in C3H10T1/2 cells on day 2, determined by real-time RT-PCR analysis. $^{**}P < 0.0001$ versus control cells. (B) Effect of Sox9 on the promoter activity of *latexin*. Data represent the fold inductions relative to the induction by mock vector transfection. $^{*}P < 0.05$ versus control cells.

strong. These findings suggest that activation of *latexin* transcription requires other transcription factors or coactivators of Sox9 such as Sox5, Sox6, and cAMP response element binding (CREB)-binding protein (CBP)/p300 [18–21].

Latexin is the only known endogenous carboxypeptidase A inhibitor in mammals [12]. It is structurally composed of two nearly identical domains that have a high conformational homology with the cystatins [22]. *Latexin* has the potential heparin/heparan sulfate-binding sites and directly interacts with a heparin component in a mast cell culture [22,16]. Heparan sulfate is an important component of the extracellular matrix of cartilage and essential for chondrocyte differentiation [23,24]. This suggests an interaction between latexin and heparan sulfate during extracellular matrix synthesis in cartilage. Our immunohistochemical study revealed the nuclear localization of latexin in chondrocytes appearing during fracture repair. It will be interesting to investigate the interaction between latexin and heparan sulfate in the nuclei, because some reports have indicated the nuclear localization of heparin sulfate [25].

In the present study, we demonstrated that latexin is expressed in chondrocytes during skeletogenesis and skeletal regeneration. *Latexin*-deficient mice, which were provided by Dr. Arimitsu [26], exhibited no growth retardation or apparent radiographic changes in the skeleton (unpublished results), suggesting the limited changes in the skeletal tissues of the mice. Since the present study revealed the dramatic upregulation of *latexin* mRNA expression in the early phase of fracture repair, it will be interesting to investigate the process of fracture repair in *latexin*-deficient mice. Such studies are currently being conducted by our group. The findings of these studies will provide important information regarding the role of latexin in skeletal growth and regeneration.

Acknowledgments

References

[1] A. Yamaguchi, T. Komori, T. Suda, Regulation of osteoblast differentiation mediated by bone morphogenetic proteins, hedgehogs, and Cbfa1, Endocr. Rev. 21 (2000) 393–411.

[2] K.S. Lee, H.J. Kim, Q.L. Li, X.Z. Chi, C. Ueta, T. Komori, J.M. Wozney, E.G. Kim, J.Y. Choi, H.M. Ryoo, S.C. Bae, Runx2 is a common target of transforming growth factor beta1 and bone morphogenetic protein 2, and cooperation between Runx2 and Smad5 induces osteoblast-specific gene expression in the pluripotent mesenchymal precursor cell line C2C12, Mol. Cell. Biol. 20 (2000) 8783–8792.

[3] M.H. Lee, Y.J. Kim, H.J. Kim, H.D. Park, A.R. Kang, H.M. Kyung, J.H. Sung, J.M. Wozney, H.M. Ryoo, BMP-2-induced Runx2 expression is mediated by Dlx5, and TGF-beta 1 opposes the BMP-2-induced osteoblast differentiation by suppression of Dlx5 expression, J. Biol. Chem. 278 (2003) 34387–34394.

[4] B.K. Zehentner, C. Dony, H. Burtscher, The transcription factor Sox9 is involved in BMP-2 signaling, J. Bone Miner. Res. 14 (1999) 1734–1741.

[5] M.B. Goldring, K. Tsuchimochi, K. Ijiri, The control of chondrogenesis, J. Cell Biochem. 97 (2006) 33–44.

[6] T. Komori, H. Yagi, S. Nomura, A. Yamaguchi, K. Sasaki, K. Deguchi, Y. Shimizu, R.T. Bronson, Y.H. Gao, M. Inada, M. Sato, R. Okamoto, Y. Kitamura, S. Yoshiki, T. Kishimoto, Targeted disruption of Cbfa1 results in a complete lack of bone formation owing to maturational arrest of osteoblasts, Cell 89 (1997) 755–764.

[7] P. Ducy, R. Zhang, V. Geoffroy, A.L. Ridall, G. Karsenty, Osf2/Cbfa1: a transcriptional activator of osteoblast differentiation, Cell 89 (1997) 747–754.

[8] C.A. Yoshida, T. Furuichi, T. Fujita, R. Fukuyama, N. Kanatani, S. Kobayashi, M. Satake, K. Takada, T. Komori, Core-binding factor beta interacts with Runx2 and is required for skeletal development, Nat. Genet. 32 (2002) 633–638.

[9] H. Akiyama, Control of chondrogenesis by the transcription factor Sox9, Mod. Rheumatol. 18 (2008) 213–219.

[10] T. Liu, Y. Gao, K. Sakamoto, T. Minamizato, K. Furukawa, T. Tsukazaki, Y. Shibata, K. Bessho, T. Komori, A. Yamaguchi, BMP-2 promotes differentiation of osteoblasts and chondroblasts in Runx2-deficient cell lines, J. Cell Physiol. 211 (2007) 728–735.

[11] Y. Arimatsu, Latexin: a molecular marker for regional specification in the neocortex, Neurosci. Res. 20 (1994) 131–135.

[12] Y. Liang, G. Van Zant, Aging stem cells, latexin, and longevity, Exp. Cell. Res. 314 (2008) 1962–1972.

[13] Y. Liang, M. Jansen, B. Aronow, H. Geiger, G. Van Zant, The quantitative trait gene latexin influences the size of the hematopoietic stem cell population in mice, Nat. Genet. 39 (2007) 178–188.

[14] E. Balint, D. Lapointe, H. Drissi, C. van der Meijden, D.W. Young, A.J. van Wijnen, J.L. Stein, G.S. Stein, J.B. Lian, Phenotype discovery by gene expression profiling: mapping of biological processes linked to BMP-2-mediated osteoblast differentiation, J. Cell Biochem. 89 (2003) 401–426.

[15] T. Katagiri, A. Yamaguchi, M. Komaki, E. Abe, N. Takahashi, T. Ikeda, V. Rosen, J.M. Wozney, A. Fujisawa-Sehara, T. Suda, Bone morphogenetic protein-2 converts the differentiation pathway of C2C12 myoblasts into the osteoblast lineage, J. Cell Biol. 127 (1994) 1755–1766.

[16] Y. Uratani, K. Takiguchi-Hayashi, N. Miyasaka, M. Sato, M. Jin, Y. Arimatsu, Latexin, a carboxypeptidase A inhibitor, is expressed in rat peritoneal mast cells and is associated with granular structures distinct from secretory granules and lysosomes, Biochem. J. 346 (Pt 3) (2000) 817–826.

[17] Y. Hatanaka, Y. Uratani, K. Takiguchi-Hayashi, A. Omori, K. Sato, M. Miyamoto, Y. Arimatsu, Intracortical regionality represented by specific transcription for a novel protein, latexin, Eur. J. Neurosci. 6 (1994) 973–982.

[18] H. Akiyama, M.C. Chaboissier, J.F. Martin, A. Schedl, B. de Crombrugghe, The transcription factor Sox9 has essential roles in successive steps of the chondrocyte differentiation pathway and is required for expression of Sox5 and Sox6, Genes Dev. 16 (2002) 2813–2828.

[19] T. Furumatsu, M. Tsuda, K. Yoshida, N. Taniguchi, T. Ito, M. Hashimoto, H. Asahara, Sox9 and p300 cooperatively regulate chromatin-mediated transcription, J. Biol. Chem. 280 (2005) 35203–35208.

[20] T. Ikeda, S. Kamekura, A. Mabuchi, I. Kou, S. Seki, T. Takato, K. Nakamura, H. Kawaguchi, S. Ikegawa, U.I. Chung, The combination of SOX5, SOX6, and SOX9 (the SOX trio) provides signals sufficient for induction of permanent cartilage, Arthritis. Rheum. 50 (2004) 3561–3573.

[21] Y. Han, V. Lefebvre, L-Sox5 and Sox6 drive expression of the aggrecan gene in cartilage by securing binding of Sox9 to a far-upstream enhancer, Mol. Cell. Biol. 28 (2008) 4999–5013.

[22] A. Aagaard, P. Listwan, N. Cowieson, T. Huber, T. Ravasi, C.A. Wells, J.U. Flanagan, S. Kellie, D.A. Hume, B. Kobe, J.L. Martin, An inflammatory role for the mammalian carboxypeptidase inhibitor latexin: relationship to cystatins and the tumor suppressor TIG1, Structure 13 (2005) 309–317.

[23] E. Arikawa-Hirasawa, H. Watanabe, H. Takami, J.R. Hassell, Y. Yamada, Perlecan is essential for cartilage and cephalic development, Nat. Genet. 23 (1999) 354–358.

[24] H.P. Sørensen, R.R. Vivès, C. Manetopoulos, R. Albrechtsen, M.C. Lydolph, J. Jacobsen, J.R. Couchman, U.M. Wewer, Heparan Sulfate Regulates ADAM12 through a molecular switch mechanism, J. Biol. Chem. 283 (2008) 31920–31932.

[25] M. Kobayashi, Y. Naomoto, T. Nobuhisa, T. Okawa, M. Takaoka, Y. Shirakawa, T. Yamatsuji, J. Matsuoka, T. Mizushima, H. Matsuura, M. Nakajima, H. Nakagawa, A. Rustgi, N. Tanaka, Heparanase regulates esophageal keratinocyte differentiation through nuclear translocation and heparan sulfate cleavage, Differentiation 74 (2006) 235–243.

[26] M. Jin, M. Ishida, Y. Katoh-Fukui, R. Tsuchiya, T. Higashinakagawa, S. Ikegami, Y. Arimatsu, Reduced pain sensitivity in mice lacking latexin, An inhibitor of metallocarboxypeptidases, Brain Res. 1075 (2006) 117–121.
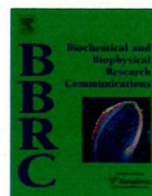
Bone morphogenetic proteins are involved in the pathobiology of synovial chondromatosis

Shoichi Nakanishi [a,d], Kei Sskamoto [a], Hiroyuki Yoshitake [b], Koji Kino [c], Teruo Amagasa [b], Akira Yamaguchi [a,d,*]

[a] Section of Oral Pathology, Graduate School of Tokyo Medical and Dental University, 1-5-45 Yushima, Bunkyo-ku, Tokyo 113-8549, Japan
[b] Section of Maxillofacial Surgery, Tokyo Medical and Dental University, Tokyo, Japan
[c] Section of Temporomandibular Joint and Occlusion, Graduate School of Tokyo Medical and Dental University, Tokyo, Japan
[d] Global Center of Excellence (GCOE) Program, International Research Center for Molecular Science in Tooth and Bone Diseases, Tokyo Medical and Dental University, Tokyo, Japan

ARTICLE INFO

ABSTRACT

Synovial chondromatosis is characterized by the formation of osteocartilaginous nodules (free bodies) under the surface of the synovial membrane in joints. Free bodies and synovium isolated from synovial chondromatosis patients expressed high levels of *BMP-2* and *BMP-4* mRNAs. BMP-2 stimulated the expression of *Sox9*, *Col2a1*, and *Aggrecan* mRNAs in free-body and synovial cells and that of *Runx2*, *Col1a1*, and *Osteocalcin* mRNAs in the free-body cells only. BMP-2 increased the number of alcian blue-positive colonies in the free-body cell culture but not in the synovial cell culture. Noggin suppressed the expression of *Sox9*, *Col2a1*, *Aggrecan*, and *Runx2* mRNAs in both the free-body and synovial cells. Further, it inhibited *Osteocalcin* expression in the synovial cells. These results suggest that BMPs are involved in the pathobiology of cartilaginous and osteogenic metaplasia observed in synovial chondromatosis.

© 2009 Elsevier Inc. All rights reserved.

Synovial chondromatosis is characterized by the formation of osteocartilaginous nodules (free bodies) under the surface of the synovial membrane in joints [1]. This disease occurs most commonly in the knee joints [1] and occasionally in the temporomandibular joint [2,3]. Although clonal karyotypic abnormalities [4,5] and rare malignant changes [6,7] have been reported in synovial chondromatosis, this disease is generally considered to be a metaplastic, and not a neoplastic, disease of synovial cells. However, the precise pathobiology involved in cartilaginous metaplasia in this disease has not been elucidated.

Mesenchymal stem cells differentiate into various types of mesenchymal cells such as osteoblasts, chondrocytes, adipocytes, and muscle [8]. During the differentiation of these cells, various local factors are involved in determining cell lineage by the regulation of lineage-specific transcription factors [9]. In the case of chondrocyte differentiation, bone morphogenetic proteins (BMPs) activate Sox9 [10], which is an essential transcription factor for chondrocyte differentiation [11,12]. BMPs also stimulate osteoblast differentiation by regulating Runx2 [8,13], which is an essential transcription factor for osteoblast differentiation [13,14]. Further,

BMP-2 converts the differentiation pathway of myogenic cells to osteoblast lineage cells by inhibiting the MyoD family transcription factors [15] and activating Runx2. Thus, BMPs play critical roles in the differentiation of various types of mesenchymal cells from mesenchymal stem cells. It has been demonstrated that synovial tissues express BMP-2, BMP-6, and BMP-7 in chronic arthritis [16–18]. Several lines of evidence indicate that synovial fibroblasts are capable of differentiating into chondrocytes by stimulation of BMPs [19–21]. These results suggest that synovial cells express BMPs under pathological conditions, and these BMPs induce the differentiation of synovial cells into chondrocytes. This prompted us to explore the role of BMPs in the pathobiology of synovial chondromatosis.

In the present study, we investigated the role of BMPs in regulating chondrocyte differentiation by using cells isolated from synovial chondromatosis patients. Here, we propose that BMPs are involved in the pathobiology of synovial chondromatosis. Our results also provide evidence that BMPs play important roles in mesenchymal cell differentiation not only in the normal developmental process but also under pathological conditions.

Materials and methods

Samples. Synovium and enucleated free bodies were obtained from two synovial chondromatosis patients, who visited the Dental

* Corresponding author. Address: Section of Oral Pathology, Graduate School of Tokyo Medical and Dental University, 1-5-45 Yushima, Bunkyo-ku, Tokyo 113-8549, Japan. Fax: +81 3 5803 0188.
    E-mail address: akira.mpa@tmd.ac.jp (A. Yamaguchi).

Hospital at Tokyo Medical and Dental University. These patients had synovial chondromatosis in the temporomandibular joint. Written informed consent was obtained from both the patients, and the experiments were approved by the hospital's Ethical Review Board.

BMP production by the synovium and free bodies in synovial chondromatosis. BMPs were detected by reverse transcription-polymerase chain reaction (RT-PCR) and immunohistochemistry. For the RT-PCR analysis, total RNA was extracted from unfixed frozen samples of the synovium and free bodies maintained at −80 °C and from cultured synovial cells by using NucleoSpin (Macherey-Nagel, Duren, Germany). RNA aliquots were reverse transcribed to complementary DNAs by using Oligo(dT) primer (Roche, Mannheim, Germany), deoxynucleotide triphosphate (dNTP; Promega), and Moloney murine leukemia virus (M-MuLV) reverse transcriptase (Fermentas, Hanover, MD). The complementary DNA products were subjected to PCR amplification, using gene-specific primers for *BMP-2*, *BMP-4*, *BMP-6*, and *BMP-7* (Table 1). The amplified products were electrophoresed on 2% agarose gel containing ethidium bromide, using OneSTEP ladder 100 (Nippon Gene, Japan).

For immunohistochemistry, synovium and a few enucleated free bodies were fixed in 10% phosphate-buffered formalin and embedded in paraffin. The free bodies were decalcified by treatment with 10% ethylenediaminetetraacetic acid (EDTA) at 4 °C for 1 week before embedding in paraffin. The embedded specimens were cut into 4 μm sections. Endogenous peroxidase activity was blocked with 10% hydrogen peroxidase/methanol, and nonspecific binding was blocked with 10% horse serum. Antigen retrieval was performed by incubating the specimens in an antigen retrieval buffer (10 mM Tris, 1 mM EDTA; pH 9.0) in a microwave at 80 °C for 60 min. The sections were incubated with goat anti-BMP-2/BMP-4 antibody (dilution, 1:500; Santa Cruz Biotechnology, Santa Cruz, CA), which specifically recognizes both BMP-2 and BMP-4. Anti-goat immunoglobulin G (IgG) (Vector laboratories, Burlingame, CA) was used as the secondary antibody. The antigen-bound peroxidase activity was visualized using 3,3′-diaminobenzidine chromogen.

Cell culture. To isolate cells from the free bodies and synovium obtained from our two patients, each tissue was cut into small pieces (approximately less than 1 × 1 mm), and the pieces were treated with 0.25% trypsin–EDTA solution at 37 °C for 20 min. After washing with phosphate-buffered saline (PBS) and Dulbecco's modified minimum essential medium (DMEM; Nacalai Tesque, Kyoto, Japan), the cells were re-incubated with DMEM containing 0.15% collagenase (Collagenase type II; Worthington Biochemical Corporation, Lakewood, NJ) and 0.25% trypsin (Becton, Dickinson and Company, Franklin Lakes, NJ) at 37 °C for 4 h. The harvested cells were inoculated into 24-well plates at a density of 2.0×10^4 cells per well and cultured in DMEM containing 10% fetal bovine serum (Invitrogen/Gibco, Carlsbad, CA), penicillin G (50 U/ml),

and streptomycin (50 mg/ml). The culture medium was changed every 3 days and maintained for 6 days with or without 500 ng/ml of recombinant human BMP-2 (rhBMP-2), which was provide by Astellas Pharma, Inc., Tokyo, Japan. To investigate the role of BMPs in chondrocyte and osteoblast differentiation, the cells isolated from the free bodies and synovium were cultured in the presence or absence of 500 ng/ml of noggin (R&D Systems, Minneapolis, MN).

RT-PCR analysis. Total RNA was extracted from the cultured cells and RNA aliquots were reverse transcribed to complementary DNAs as described above. The complementary DNA products were subjected to PCR amplification, using gene-specific primers for *Sox9*, *Col1a1*, *Col2a1*, *Col10a1*, *Aggrecan (Agc1)*, *Runx2*, and *Osteocalcin* (Table 1). Real-time RT-PCR amplification was performed using a LightCycler System (Roche) with a Platinum SYBR Green qPCR SuperMix UDG kit (Invitrogen, Carlsbad, CA). The relative amount of each mRNA was normalized to *β-actin* mRNA.

Histochemical staining. Cultured cells were fixed in 10% phosphate-buffered formalin for 5 min, washed twice with 10 mM Tris–HCl (pH 7.5), and then double stained with alkaline phosphatase (ALP) and alcian blue. ALP staining was performed at 37 °C for 20 min by using 2-(4-iodophenyl)-3-(4-nitrophenyl)-5-phenyl-2*H*-tetrazolium chloride (INT) as a formazan dye with 5-bromo-4-chloro-3-indolyl phosphate (BCIP) as an enhancer (Roche). After the ALP staining, alcian blue (pH 2.5) staining was performed. Alcian blue-positive nodules were defined as those having a diameter of more than 50 μm.

Measurement of ALP activity. Cultured cells were sonicated in radioimmunoprecipitation assay (RIPA) buffer to obtain the cell lysate. ALP activity was determined using *p*-nitrophenylphosphate solution (Wako Pure Chemicals, Osaka, Japan) as the substrate. The amount of *p*-nitrophenylphosphate released was estimated by measuring the absorbance at 405 nm after 30 min of incubation at 37 °C. The protein concentration was determined using a bicinchoninic acid (BCA) protein assay kit (Thermo, Waltham, MA).

Statistical analyses. We used *t*-test for the statistical analysis of the influence of rhBMP-2 and noggin. *P* values less than 0.05 were considered significant. Each analysis was performed at least 3 times. The data are presented as mean ± standard error of mean (SEM) of independent replicates ($n \geqslant 3$).

Results and discussion

The synovium and free bodies expressed BMPs in synovial chondromatosis

In synovial chondromatosis, free bodies were produced in the joints (Fig. 1A), which are composed of cartilaginous tissues (Fig. 1B). We hypothesized that the synovium and free bodies synthesized BMPs, which might be involved in the excess formation of

Table 1
Primers sequences used for RT-PCR.

| Gene	Forward primer	Reverse primer
BMP-2	5′-GCAGTGCTACTGTTGAG	3′-AGATCAGCAATGTCTGGT
BMP-4	5′-AAGCGTAGCCCTAAGCATCA	3′-TGGTTGAGTTGAGGTGGTCA
BMP-6	5′-GCGACACCACAAAGAGTTCA	3′-CCCATACTACACGGGTGTCC
BMP-7	5′-GGTCATGAGCTTCGTCAACC	3′-GCAGGAAGAGATCCGATTCC
Sox9	5′-AGCAAAGGAGATGAAATCTGTTCTG	3′-AGAGTCTTGTGGTCGTCAATTGGA
Aggrecan	5′-AAGTATCATCAGTCCCAGAATCTAGCA	3′-TTGGTGGAGACGTAAGGTGC
Col1a1	5′-CACCAATCACCTGCGTACAGAA	3′-CAACACGCTACTGCACTAGACA
Col2a1	5′-CGAGTACCGATCACAGA	3′-ACTGCGGTTAGAAAGTATTTG
Col10a1	5′-GCCCGATCTTGTGTGC	3′-CTTACCTGCGTGCTGG
Runx2	5′-AGAAGGCACAGACAGAAGCTTGA	3′-TCACTAAATCCCGCGTAAGGA
Ocn	5′-GGCAGCGAGGTAGTGAAGAG	3′-CTGGAGAGGAGCAGAACTGG
β-Actin	5′-AAACTGGAACGGTGAAGGTG	3′-TCAAGTTGGGGGACAAAAAG
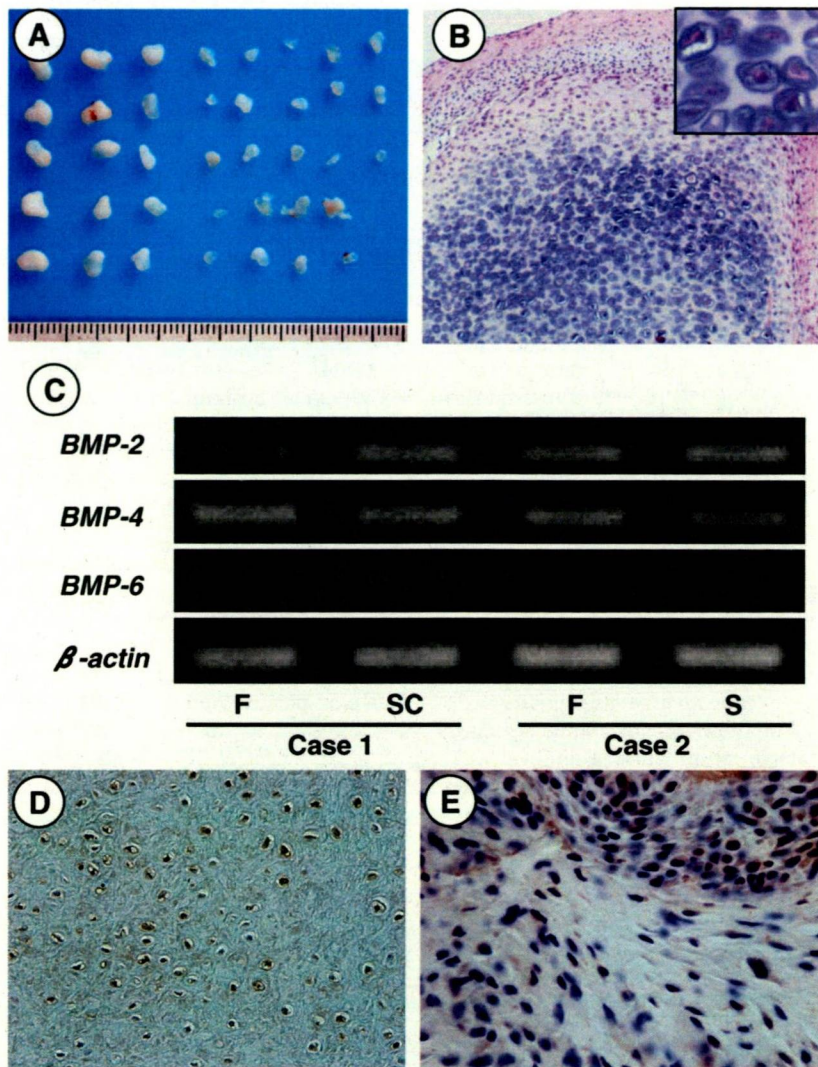
Fig. 1. Free bodies and BMP expression in synovial chondromatosis. (A) Gross findings of free bodies used for isolation of culture cells. Thirty-eight enucleated nodules were isolated from the temporomandibular joint in one patient. (B) Typical histology of a free body, which is composed of hyaline cartilage. Right upper insert shows a high magnification view of cartilage. (C) Expression of BMP-2, BMP-4, and BMP-6 mRNAs in the free bodies (F) and synovium (S) or cultured synovial cells (Sc). RT-PCR analysis was performed as described in Materials and methods. (D,E) Immunohistochemical detection of BMP-2/BMP-4 in the free bodies (D) and synovium (E). Immunoreactivity (brown) is seen in chondrocytes (D) and some fibroblastic cells (E). Immunohistochemistry was performed as described in Materials and methods.

cartilage or bone in synovial chondromatosis. To corroborate our hypothesis, we first investigated BMP expression in the synovium or cultured synovial cells and the free bodies isolated from two synovial chondromatosis patients. RT-PCR analysis revealed that the synovium or cultured synovial cells and the free bodies expressed high levels of BMP-2 and BMP-4 mRNAs (Fig. 1C). BMP-6 expression was weak in the free bodies and undetectable in the synovium or cultured synovial cells (Fig. 1C). No apparent BMP-7 expression was detected in either the synovium or the free bodies. Immunohistochemical study demonstrated that chondrocytes in the free bodies (Fig. 1D) and some fibroblastic cells in the synovium (Fig. 1E) expressed BMP-2/BMP-4. These results indicate the production of BMP-2 and BMP-4 by the free bodies and synovium in synovial chondromatosis and suggest the possible involvement of BMPs in the pathobiology of synovial chondromatosis. These results prompted us to further investigate the effects of rhBMP-2 on chondrogenic and osteogenic differentiation in the free-body and synovial cells isolated from synovial chondromatosis patients.

rhBMP-2 stimulated the production of cartilaginous nodules and ALP-positive cells in the culture of cells isolated from synovial chondromatosis patients

We first assessed the effects of rhBMP-2 on chondrogenic and osteogenic differentiation of cells by dual staining with ALP and alcian blue in the cells isolated from the free bodies and synovium. In the culture of free-body cells isolated from Case 1, we found numerous nodules composed of spherical cells associated with alcian blue-positive extracellular matrices, indicating chondrogenic differentiation (Fig. 2A). BMP-2 treatment (500 ng/ml) for 6 days increased the number of these nodules by 1.5 times than that in the BMP-2-untreated culture (Fig. 2B). Free-body cells isolated from Case 2 formed a few such nodules (Fig. 2B). Cultured synovial cells exhibited no apparent alcian blue-positive nodules in the presence or absence of BMP-2 (data not shown). These results indicate that free-body cells are capable of differentiating into chondrocytes more effectively than synovial cells.
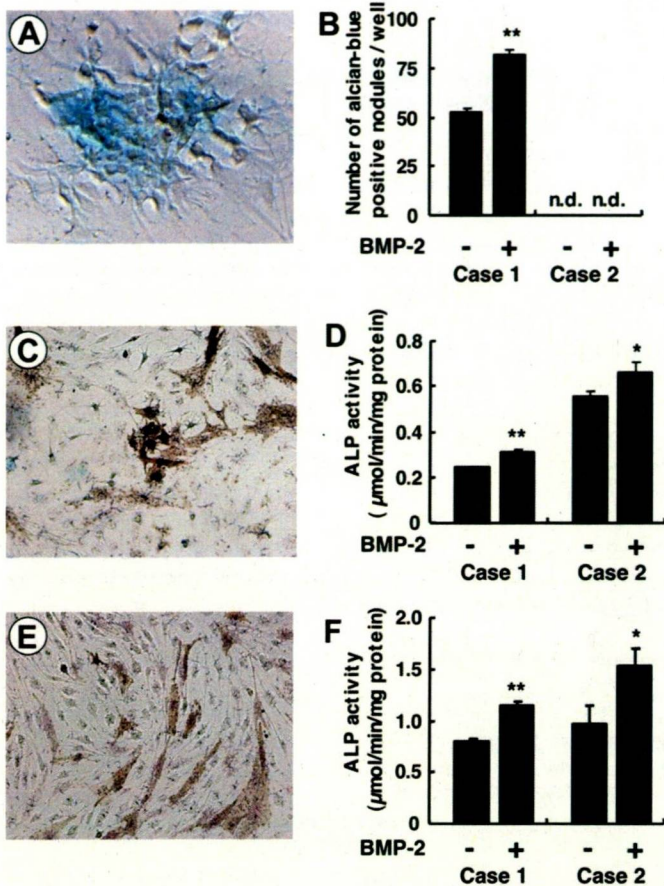
Fig. 2. Effects of rhBMP-2 on cartilaginous nodule formation (A, B) and ALP activity (C–F). (A) Double staining of the cultured cells isolated from the free bodies with ALP and alcian blue in the presence of rhBMP-2. Note that round-shaped alcian blue-positive cells (blue) form a cartilaginous colony. No ALP-positive cells are observed. (B) The number of alcian blue-positive colonies observed in culture of free-body cells and synovial cells in the presence or absence of rhBMP-2 (500 ng/ml). No positive colonies were observed in the synovial cell culture. (C, E) ALP histochemistry in free-body cells (C) and synovial cells (E). Numerous ALP-positive cells (brown) were observed in the cultures of free-body and synovial cells in the presence of rhBMP-2. (D, F) ALP activity in the free-body cells (D) and synovial cells (F) cultured with or without rhBMP-2.

ALP-positive cells were scattered in the cultures of both free-body (Fig. 2C) and synovial cells (Fig. 2E). Almost all the cells were polyhedral or spindle-shaped without any close association with the alcian blue-positive nodules (Fig. 2C and E). BMP-2 treatment increased the number of ALP-positive cells in the cultures of both the free-body and synovial cells (data not shown). Further, BMP-2 treatment significantly increased ALP activity in both the free-body cells (Fig. 2D) and the synovial cells (Fig. 2F). ALP activity is exhibited from early differentiated osteoblasts through mature osteoblasts [8], but it appears in only mature hypertrophic cells during chondrocyte differentiation. We found few nodules double-positive for ALP and alcian blue even in the cultures treated with rhBMP-2. These suggest that ALP-positive polyhedral or spindle-shaped cells are osteoblast lineage cells.

BMP-2 stimulated the expression of mRNAs related to chondrocyte and osteoblast differentiation in the culture of cells isolated from synovial chondromatosis patients

We investigated the effects of rhBMP-2 on the expression of mRNAs related to chondrocyte differentiation. The basal expres-

sion levels of *Sox9*, *Col2a1*, *Aggrecan*, and *Col10a1* mRNAs were significantly higher in the free-body cells than in the synovial cells (data not shown). BMP-2 treatment increased *Sox9* mRNA expression over 20-fold in the free-body cells (Fig. 3A). BMP-2 also significantly increased the expression of *Col12a1* and *Aggrecan* mRNAs, which are involved in the early differentiation of chondrocytes [22] (Fig. 3A). The expression of *Col10a1* mRNA, which is mainly expressed by hypertrophic chondrocytes [22], was also stimulated by the BMP-2 treatment, but its induction in the treated culture was less than 2-fold as compared with that in the control cultures (Fig. 3A). In the synovial cells, rhBMP-2 treatment significantly increased the expression of *Sox9*, *Col2a1*, and *Aggrecan* mRNAs (Fig. 3B). BMP-2 increased *Col10a1* expression more effectively in the synovial cells than in the free-body cells. These results indicate that rhBMP-2 stimulates the free-body and synovial cells to differentiate into chondrogenic cells.

We next investigated the effects of rhBMP-2 on the expression of mRNAs related to osteoblast differentiation. BMP-2 treatment significantly increased *Runx2* expression but failed to stimulate *Co1a1* expression in the free-body cells. rhBMP-2 slightly, but significantly, increased *Osteocalcin* expression in only Case 2. In the synovial cells, BMP-2 treatment significantly increased the expression of *Runx2*, *Col1a1*, and *Osteocalcin* mRNAs. These results suggest that rhBMP-2 induces osteoblast differentiation more effectively in synovial cells than in free-body cells.

Taken together, these results indicate that BMP-2 treatment stimulates chondrocyte and osteoblast differentiation in free-body and synovial cells. Our histopathological examination of eight patients with synovial chondromatosis in the temporomandibular joint revealed that free bodies in all the cases exhibited extensive cartilage formation, and only one case was associated with bone formation (unpublished results). These findings support that the
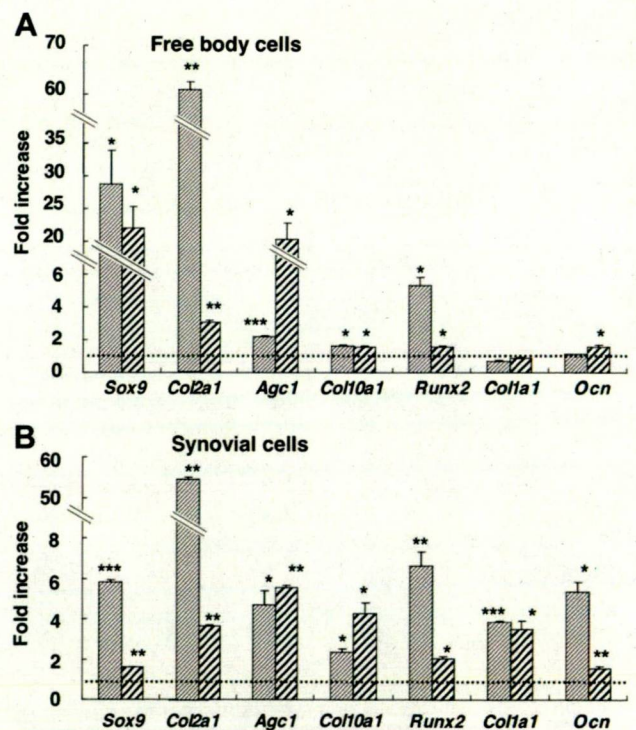

Fig. 3. Effects of BMP-2 on the expression of mRNAs related to chondrocyte and osteoblast differentiation in the free-body cells (A) and synovial cells (B). The cells were cultured for 6 days in the presence or absence of BMP-2 (500 ng/ml), and the expression of mRNAs was determined by real-time RT-PCR analysis as described in Materials and methods. Agc1, Aggrecan. Thin slash bars indicate the data of Case 1, and thick slash bars show that of Case 2. $^{*}P < 0.05$, $^{**}P < 0.01$, $^{***}P < 0.001$ ($n = 3$).

free-body cells used in the present study had differentiated into chondrogenic cells, and the synovial cells retained bipotency to differentiate into both chondrocytes and osteoblasts.

Noggin inhibited the expression of marker genes related to chondrocyte and osteoblast differentiation in the cultured cells

The free-body and synovial cells expressed substantial levels of mRNAs related to chondrocyte and osteoblast differentiation in the absence of exogenous BMP-2. We also demonstrated that the free-body and synovial cells expressed BMPs. These results suggested that endogenous BMPs synthesized by the free-body and synovial cells stimulated chondrocyte and osteoblast differentiation in an autocrine or a paracrine fashion. To address this issue, we investigated the effects of noggin, which is a specific antagonist for BMPs [23,24], on chondrogenic and osteoblastic differentiation in the free-body and synovial cells.

Noggin significantly inhibited *Sox9* and *Col2a1* expression in both the free-body and synovial cells (Fig. 4A and B). Noggin also inhibited aggrecan expression in the free-body cells but not in the synovial cells (Fig. 4A and B), which might be due to the low level of basal aggrecan mRNA expression in the latter. The inhibitory effect of noggin on *Col10a1* expression was observed in only one case each in the free-body and synovial cells (Fig. 4A and B). These results indicate that BMPs synthesized by free-body and synovial cells are involved in chondrogenic differentiation in synovial chondromatosis.

Noggin significantly inhibited *Runx2* expression in the free-body and synovial cells, but its inhibitory effect on *Col1a1* expression was observed in only synovial cells isolated from Case 1 (Fig. 4A and B). Noggin inhibited *Osteocalcin* expression in the synovial cells but not in the free-body cells (Fig. 4A and B). The ALP activity in the free-body (Fig. 4C) and synovial cells (Fig. 4D) was also inhibited by noggin. These results suggest that BMPs synthesized by free-body and synovial cells also participate in the regulation of osteoblast differentiation in synovial chondromatosis.

In conclusion, the present study demonstrated that the free bodies and synovium isolated from synovial chondromatosis patients produced BMPs and that the free-body and synovial cells are capable of differentiating into chondrocyte and osteoblast lineage cells in response to BMPs. Thus, we propose that BMPs synthesized by synovial and free-body cells promote cartilaginous and osteogenic metaplasia in synovial chondromatosis in an autocrine or a paracrine fashion. The present study also indicates that BMPs play important roles in not only skeleton formation but also in the cartilaginous and osteogenic metaplasia observed under pathological conditions. Thus, BMP antagonists such as noggin might be useful therapeutic tools for preventing chondrogenic metaplasia occurred in synovial chondromatosis.

Acknowledgments

References

[1] F.P. Murphy, D.C. Dahlin, C.R. Sullivan, Articular synovial chondromatosis, J. Bone Joint Surg. Am. 44 (1962) 77–86.
[2] V. Karlis, R.S. Grickman, M. Zaslow, Synovial chondromatosis of the temporomandibular joint with intracranial extension, Oral Surg. Oral Med. Oral Pathol. Oral Radiol. Endod. 86 (1998) 664–666.
[3] J.J. von Lindern, I. Theuerkauf, B. Niederhagen, S. Bergé, T. Appel, R.H. Reich, Synovial chondromatosis of the temporomandibular joint: clinical, diagnostic, and histomorphologic findings, Oral Surg. Oral Med. Oral Pathol. Oral Radiol. Endod. 94 (2002) 31–38.
[4] F. Mertens, K. Jonsson, H. Willén, A. Rydholm, A. Kreicbergs, L. Eriksson, G. Olsson-Sandin, F. Mitelman, N. Mandahl, Chromosome rearrangements in synovial chondromatous lesions, Br. J. Cancer 74 (1996) 251–254.
[5] R. Sciot, P. Dal Cin, J. Bellemans, I. Samson, H. Van den Berghe, V.B. Damme, Synovial chondromatosis: clonal chromosome changes provide further evidence for a neoplastic disorder, Virchows Arch. 433 (1998) 189–191.
[6] B.L. Sperling, S. Angel, G. Stoneham, V. Chow, A. McFadden, R. Chibbar, Synovial chondromatosis and chondrosarcoma: a diagnostic dilemma, Sarcoma 7 (2003) 69–73.
[7] R.L. Davis, H. Foster, K. Arthur, S. Trewin, P.W. Hamilton, D.J. Biggart, Cell proliferation studies in primary synovial chondromatosis, J. Pathol. 184 (1998) 18–23.
[8] A. Yamaguchi, T. Komori, T. Suda, Regulation of osteoblast differentiation mediated by bone morphogenetic proteins, hedgehogs, and Cbfa1, Endocr. Rev. 21 (2000) 393–411.
[9] G.A. Rodan, S. Harada, The missing bone, Cell 30 (1997) 677–680.
[10] E.J. Jin, S.Y. Lee, Y.A. Choi, J.C. Jung, O.S. Bang, S.S. Kang, BMP-2-enhanced chondrogenesis involves p38 MAPK-mediated down-regulation of Wnt-7a pathway, Mol. Cells 22 (2006) 353–359.
[11] W. Bi, J. Min Deng, Z. Zhang, R. Behringer, B. de Crombrugghe, Sox9 is required for cartilage formation, Nat. Genet. 22 (1999) 85–89.
[12] Y. Mori-Akiyama, H. Akiyama, D.H. Rowitch, B. de Crombrugghe, Sox9 is required for determination of the chondrogenic cell lineage in the cranial neural crest, Proc. Natl. Acad. Sci. USA 100 (2003) 9360–9365.
[13] P. Ducy, R. Zhang, V. Geoffroy, A.L. Ridall, G. Karsenty, Osf2/Cbfa1: a transcriptional activator of osteoblast differentiation, Cell 89 (1997) 747–754.
[14] T. Komori, H. Yagi, S. Nomura, A. Yamaguchi, K. Sasaki, K. Deguchi, Y. Shimizu, R.T. Bronson, Y.-H. Gao, M. Inada, M. Sato, R. Okamoto, Y. Kitamura, S. Yoshiki, T. Kishimoto, Targeted disruption of Cbfa1 results in a complete lack of bone formation owing to maturational arrest of osteoblasts, Cell 89 (1997) 755–764.
[15] K. Katagiri, A. Yamaguchi, K. Komaki, E. Abe, N. Takahashi, T. Ikeda, V. Rosen, J.M. Wozney, A. Fujisawa-Sehara, T. Suda, Bone morphogenetic protein-2 converts the differentiation pathway of C2C12 myoblasts into the osteoblast lineage, J. Cell. Biol. 127 (1994) 1755–1766.
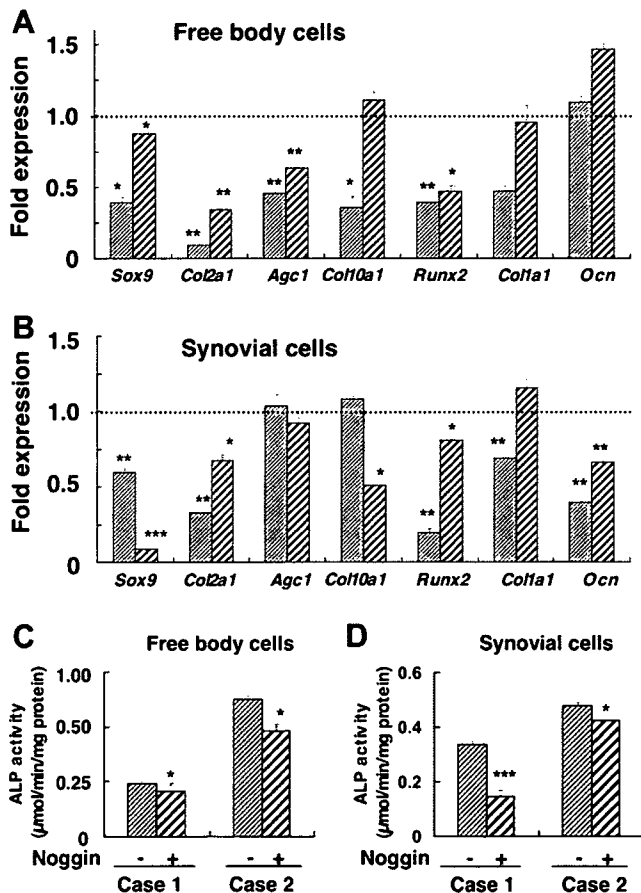

Fig. 4. Effects of noggin on the expression of mRNAs related to chondrocyte and osteoblast differentiation in the free-body cells (A) and synovial cells (B). The cells were cultured for 6 days in the presence or absence of noggin (500 ng/ml), and the expression of mRNAs was determined by real-time RT-PCR analysis as described in Materials and methods. Agc1, Aggrecan. Thin slash bars indicate the data of Case 1, and Thick slash bars show that of Case 2. $^*P < 0.05$, $^{**}P < 0.01$, $^{***}P < 0.001$ ($n = 3$).